

QATAR UNIVERSITY

COLLEGE OF ENGINEERING

INVESTIGATION OF LAMINAR FLAME SPEED  
OF ALTERNATIVE LIQUID FUEL BLENDS

BY

SAMAHAT SAMIM

A Thesis Submitted to the Faculty of  
College of Engineering  
in Partial Fulfillment of the Requirements  
for the Degree of  
Master of Science

January 2016

© 2016 Samahat Samim. All Rights Reserved.

## COMMITTEE PAGE

The members of the Committee approve the thesis of Samahat Samim defended on 19/01/2016.

---

Dr. Samer F. Ahmed  
Thesis Supervisor

---

Prof. Madjid Birouk  
Committee Member

---

Dr. Saud Ghani  
Committee Member

---

Dr. Ahmed Sleiti  
Committee Member

Approved:

---

Dr. Rashid Alammari, Dean, College of Engineering

## ABSTRACT

The rapid fluctuation in oil prices and increased demand of clean fuels to reduce emissions has forced the researchers to find alternative fuels that can give the same or better overall fuel characteristics. This thesis aims at looking into the prospects of Gas to Liquid (GTL) fuel as an alternative fuel for Internal Combustion Engines (ICEs), by investigating the flame speed of GTL fuel and its 50/50 (by volume) blend with conventional diesel. The tests were conducted in a newly designed state of the art cylindrical bomb test rig capable of measuring laminar flame speed at different initial temperatures and equivalence ratios, employing pressure signal for measuring flame speeds.

The bomb measurements for conventional diesel were found in an excellent agreement (error of 1.5%) when compared with the literature. The GTL and its 50/50 blend were investigated for their laminar flame speeds, along with the effect of changing the equivalence ratio and initial temperature on the flame speed.

It was found that the pure GTL has highest flame speed ( $S_N=88.3$  cm/s) as compared to conventional diesel, near and at stoichiometric mixtures ( $\Phi=1.1$ ), which was 5 cm/s more than conventional diesel. At lean and rich mixtures, the flame speed of GTL get slightly lower than conventional diesel. The 50/50 blend gave a lower flame speed at lean and rich mixture conditions as compared to the rest of the fuels. The

flame speed of 50/50 blend was almost the same as that of pure conventional diesel at stoichiometric conditions. The flame speed of all three tested fuels was increasing with the increase of initial temperature of the mixture, which also confirms with the literature. It was concluded that the GTL fuel is good if the application requires higher flame speed near the stoichiometric conditions. If the application requires conserving conventional diesel and using alternative fuel, 50/50 blend of conventional diesel and GTL shall give the exact flame speeds.

## TABLE OF CONTENTS

List of Figures .....	xi
List of Tables .....	xv
Nomenclature .....	xvii
Acknowledgements.....	xviii
Chapter 1. Introduction .....	1
1.1 Background and Justification .....	1
1.1.1 Need for Alternative Fuels.....	1
1.1.2 Environment and Role of Qatar .....	2
1.1.3 GTL as Alternative Fuel .....	3
1.1.4 GTL and Role of Qatar .....	4
1.1.5 Scope of Present Work .....	5
1.2 Project Aim and Objectives.....	6
1.3 Project Methodology .....	7
Chapter 2. Literature Review .....	9

2.1 Gas-To-Liquid (GTL) as Alternative Fuel.....	9
2.1.1 Introduction to GTL.....	9
2.1.2 GTL Production Process .....	10
2.1.3 Previous Research Work on GTL.....	12
2.2 Flame Speed.....	14
2.3 Test Rigs for Flame Speed Measurements .....	15
2.3.1 Slot Burner Method .....	16
2.3.2 Bunsen Burner Method .....	17
2.3.3 Tube Propagation Method.....	19
2.3.4 Soap Bubble Method .....	20
2.3.5 Constant Volume Bomb Method .....	21
2.4 Previous Research Work using Bomb Method .....	22
Chapter 3. Test Rig Designing & Fabrication .....	30
3.1 Proposed Experimental Method.....	30
3.2 Cylindrical Bomb Test Rig Designing and Manufacturing.....	33

3.2.1 Design and Fabrication Process – Phase One .....	33
3.2.2 Pending Works on Test Rig for Phase Two .....	37
3.3 Test Rig Developments and Modifications – Phase Two .....	38
3.3.1 Installation of Control Boards and Components .....	38
3.3.2 Spark Coil Ignition System Installation .....	40
3.3.3 Pressure Transducer Components and Installation.....	42
3.3.4 Installation of Heating Coils .....	46
3.3.5 Vacuum Pump and Compressor Installation .....	49
3.3.6 Lambda Sensor Installation.....	50
3.3.7 Safety Concerns and Modifications to the Test Rig.....	51
3.4 Final Test Rig Design .....	53
Chapter 4. Experimental SETUP and Procedure .....	55
4.1 Test Rig Characterization .....	55
4.1.1 Calibration of Thermocouple .....	56
4.1.2 Maximum Temperature Testing .....	56

4.1.3 Calibration of Pressure Transducer .....	58
4.1.4 Setting up the Oscilloscope (DAQ).....	58
4.1.5 Pressure Leakage Testing.....	61
4.2 Final Experimental Procedure.....	64
4.3 Fuels Used .....	66
4.4 Flame Visualization Experiment.....	66
Chapter 5. Results and Discussion .....	68
5.1 Conventional Diesel .....	68
5.1.1 Pressure Sensor Data Interpretation for Diesel Tests .....	69
5.1.2 Equivalence Ratio Calculations for Diesel Tests .....	71
5.1.3 Summary of Results for Equivalence Ratios from Diesel Fuel Tests.....	74
5.1.4 Flame Speed Calculations for Diesel Tests.....	75
5.3.1 Summary of Results for Flame Speed for Diesel Tests .....	76
5.2 Validation of Results using Diesel Tests.....	78
5.2.1 Comparison with Existing Work.....	78



5.2.2 Repeatability Test .....	80
5.3 Pure GTL.....	81
5.3.1 Summary of Results for GTL Tests .....	81
5.3.2 Effect of Varying the Equivalence Ratio of GTL .....	82
5.3.3 Effect of Varying the Initial Temperature of GTL.....	83
5.4 GTL and Conventional Diesel Blend .....	84
5.4.1 Summary of Results for 50/50 Blend Tests.....	85
5.4.2 Effect of Varying the Equivalence Ratio 50/50 Blend.....	85
5.4.3 Effect of Varying the Initial Temperature of 50/50 Blend .....	86
5.5 Comparison of Results for the Tested Fuels .....	87
5.5.1 Effect of Equivalence Ratio Variation on the Flame Speed .....	87
5.5.2 Effect of Initial Temperature Variation on the Flame Speed.....	89
Chapter 6. ConclusionS and Recommendations.....	92
6.1 Conclusions .....	92
6.2 Recommendations .....	94

References .....	95
Appendix A: MS Excel Equivalence Ratio Calculator .....	103
Appendix B: MS Excel Flame Calculator.....	105
Appendix C: Calibration Certificates .....	106
Appendix D: GTL MSDS .....	110

## LIST OF FIGURES

Figure 1 - Project methodology flow chart.....	7
Figure 2 - GTL production process .....	11
Figure 3 - Slot burner method .....	16
Figure 4 - Bunsen burner method .....	18
Figure 5 - Tube propagation method .....	19
Figure 6 - Soap bubble method .....	20
Figure 7 - Spherical bomb method schematic .....	23
Figure 8 - Mk2 combustion bomb at University of Leeds.....	26
Figure 9 - Plot of flame speed vs. flame radius .....	27
Figure 10 - Cylindrical bomb test rig by Radwan .....	28
Figure 11 - Results of experimental study by Radwan .....	29
Figure 12 - Schematic of proposed test rig.....	31
Figure 13 - Sketch of bomb shell, flanges and windows sketch .....	33
Figure 14 - Bomb and stand manufacturing .....	34

Figure 15 - Windows and ports installation.....	35
Figure 16 - Fans design and installation.....	35
Figure 17 - Fan shaft sealing design.....	36
Figure 18 - Spark electrode system .....	37
Figure 19 - Control board components installation.....	39
Figure 20 - Spark ignition system diagram.....	40
Figure 21 - Spark ignition system components.....	41
Figure 22 - Spark between two electrodes.....	41
Figure 23 - Taping hole and machined adapter .....	42
Figure 24 - Pressure transducer mounting .....	43
Figure 25 - Omega pressure transducer testing .....	44
Figure 26 - PCB pressure transducer and PCB charge converter.....	45
Figure 27 - PCB pressure sensor setup .....	45
Figure 28 - GW-Instek oscilloscope.....	46
Figure 29 - Four heating coils.....	47

Figure 30 - Installation of heating coils.....	48
Figure 31 - Vacuum pump connection.....	49
Figure 32 - Air Compressor .....	50
Figure 33 - Lambda sensor piping and connection.....	51
Figure 34 - Final test rig design after modifications .....	53
Figure 35 - Thermocouple Calibration .....	56
Figure 36 - Temperature vs. time testing .....	57
Figure 37 - Pressure sensor calibration .....	58
Figure 38 - Oscilloscope reader display settings.....	60
Figure 39 – MS Excel solver for moles of air at 20oC, 180oC and 200oC.....	63
Figure 40 - Flame visualization.....	67
Figure 41 - Raw signal of pressure .....	70
Figure 42 - Pressure vs. time plot for diesel at 180 °C.....	70
Figure 43 - Results for pure diesel ( $S_N$ vs. $\Phi$ ) .....	77
Figure 44 - Test rig results validation.....	79

Figure 45 - Results of GTL ( $S_N$ vs. $\Phi$ ) .....	82
Figure 46 - Results of 50-50 blend ( $S_N$ vs. $\Phi$ ) .....	86
Figure 47 - Conventional Diesel, GTL and 50-50 Blend ( $S_N$ vs. $\Phi$ ) .....	88
Figure 48 - Effect of changing initial temperature for GTL and 50-50 blend.....	90

## LIST OF TABLES

Table 1 - Worldwide production of GTL products .....	4
Table 2 - Properties of GTL products .....	12
Table 3 - Numerical models for flame speed.....	25
Table 4 - Oscilloscope settings.....	59
Table 5 - Pressure leakage testing results .....	63
Table 6 - Properties of fuels used .....	66
Table 7 - Test details .....	69
Table 8 - Equivalence ratio calculations summary - diesel.....	74
Table 9 - Equations for flame speed calculation .....	75
Table 10 - Flame speed calculations .....	76
Table 11 - Diesel test results summary.....	77
Table 12 - Repeatability test results .....	80
Table 13 - GTL test results summary.....	82
Table 14 – GTL initial temperature variation.....	83

Table 15 – 50-50 blend results summary.....	85
Table 16 – 50-50 blend initial temperature variation.....	87
Table 17 - Effect of initial temperature variation .....	90



## NOMENCLATURE

$\Phi$	Equivalence Ratio	$\rho_{\text{air}}$	Density of air
$S_N$	Laminar Flame Speed	$\rho_{\text{fuel}}$	Density of fuel
$S_T$	Turbulent Flame Speed	$R_{\text{bomb}}$	Radius of bomb
$\rho$	Density	$r_i$	Instantaneous radius before combustion
$P$	Pressure	$r_b$	Instant radius after combustion
$T$	Temperature	$P_i$	Initial pressure before combustion
$V$	Volume	$P_e$	Equilibrium pressure
$R$	Ideal Gas Constant	$T_u$	Temperature of burnt gases
$n_{\text{air}}$	Moles of air	$T_i$	Initial temperature of mixture
$n_{\text{fuel}}$	Moles of fuel	$\gamma_u$	Specific Heat Ratio
$n_{\text{o}_2}$	Moles of oxygen	EES	Engineering Equation Solver
$n_{\text{N}_2}$	Moles of nitrogen	ICE	Internal Combustion Engine
$m_{\text{air}}$	Mass of air	DAQ	Data Acquisition System
$M.M_{\text{air}}$	Molar mass of air	GTL	Gas To Liquid
$m_{\text{fuel}}$	Mass of fuel	FT	Fischer Tropsch
$M.M_{\text{fuel}}$	Molar mass of fuel	QU	Qatar University
$(A/F)_{\text{stoic}}$	Stoichiometric air to fuel ratio	STP	Standard Temperature and Pressure
$(A/F)_{\text{act}}$	Stoichiometric air to fuel ratio		
$V_{\text{fuel}}$	Volume of fuel		
$V_{\text{air}}$	Volume of air		

## **ACKNOWLEDGEMENTS**

First, I would like to thank Allah (God) Almighty for providing me the courage and the blessing to complete this project.

I am sincerely grateful to all who supported me in completing this project effectively and on time. I put forward my utmost appreciation to my project supervisor, Dr. Samer F. Ahmed, for his counseling and advice throughout the project. Dr. Samer suggested the project idea and provided his extreme moral and technical support in the form lectures, tutorials and project meetings and I thank him again for his assistance.

In addition, I would like to thank Eng. Yehya and Mr. Roy from Qatar University Mechanical Workshop for helping me out in building the test rig and carrying out the experimental tests for this project. I would like to extend my sincere gratitude to the teaching staff, library staff and my batch mates at the Qatar University for their support in this project.

Finally yet importantly, I would like to thank my dear parents and my beloved wife, who have extended their support for enabling me to study and helping me out morally and financially in this endeavor.

## **CHAPTER 1. INTRODUCTION**

This chapter of the thesis starts by giving the background and justification for the suggested thesis topic. The current trends and need for this study is given, highlighting the role of Qatar in the GTL industry and its research. Lastly, based on the given justification, project aim and objectives were given.

### **1.1 Background and Justification**

#### **1.1.1 Need for Alternative Fuels**

In 1973, the oil crisis resulting in very high prices of crude oil as well as lack of supply, forced many countries to look for alternative fuels for replacing the conventional fuels at use during that time [1]. A safer approach applied at that time was to search for alternative fuels that can be used either purely or in blended form with the conventional fuel. This, of course, will be to reduce the demand of conventional fuel and at the same time, increase the performance characteristics and reduce emissions of the combustion in engines and gas turbines.

Also, in the past 20 years, there has been a great deal of research and measures taken to minimize the environmental damages done by human due to industrial development. One such area, which needs attention, is the phenomena of global

warming. Human activities like excessive use of non-renewable sources, stack waste and ICE emissions can promote global warming and accelerate the climate change in a destructive way and there is a need to control it [2]. The tough legislations in European Union and USA to reduce emissions have pushed the different industries to look into alternative fuels with less emissions.

### **1.1.2 Environment and Role of Qatar**

Qatar has experienced a phenomenal growth in industry, especially related to Oil and Gas. This rapid growth instills a great responsibility on Qatar to protect the environment at any scale. According to Qatar National Vision 2030:

“The State shall preserve the environment and its natural balance in order to achieve comprehensive and sustainable development for all generations” [3]

In the Qatar National Vision 2030, environmental development has been considered one of four major pillars on which the future of Qatar will be based. Also the need to address the global environmental issues of global warming has been directly highlighted in the 2030 vision. Qatar is one of the largest producers of Natural Gas and CO<sub>2</sub> is one of the byproducts of this process. According to Whitson and Kuntadi [4], the annual production of CO<sub>2</sub> in Qatar is 2.54 million metric tons. Along with this, there is significant amount of CO<sub>2</sub> being produced in burning of fossil fuel and coal for the production of electricity, cement production and many other industrial

processes.

There is a great potential of global warming in Qatar and therefore this issue needs to be addressed by all the industries as well as the government of Qatar. Also, there is a need to look into cleaner alternative fuels with reduced emissions to minimize the environmental damage by global warming.

### **1.1.3 GTL as Alternative Fuel**

This demand for alternative fuels requires from the researchers to thoroughly investigate the combustion properties of the alternative fuels in comparison with the existing conventional fuels. One such alternative fuel that has gained much interest recently is the Gas-To-Liquid (GTL) products.

A very recent detailed review paper published by Sajjad *et. al.* [5], conducts a detailed analysis of GTL fuel blends with conventional diesel by studying the fuel characteristics, combustion behavior, its effect on engine performance and emissions. The paper concludes by reviewing various studies of GTL fuel blends that the GTL fuel can be safely regarded as a cleaner fuel with much reduced emission and greenhouse effect. Also, the same research established that the power of an engine using conventional diesel increase about 1% to 5% when used with GTL.

### 1.1.4 GTL and Role of Qatar

Qatar is one of the primary producer and exporter of GTL products. In 2006, the Government of the State of Qatar approved the project plan of the largest GTL plant of the world, Pearl GTL. By 2011, Qatar had two GTL plants developed and ready for production.

Table 1 shows the contribution of Qatar in the production of GTL products and it can be seen clearly that Qatar is by far, the largest producer of GTL products.

*Table 1 - Worldwide production of GTL products [6]*

Name	Pearl GTL plant	Oryx GTL Plant	Oltin YO'l GTL Plant	Escravos gas to Liquids (EGTL) Plant	Westlake GTL project	Canada GTL project
<b>Location</b>	Ras Laffan Industrial City, Qatar	Ras Laffan Industrial City, Qatar	Qarshi, Uzbekistan	Escravos, Nigeria	Westlake, Calcasieu Parish, Louisiana, USA	Alberta's Industrial Heartland, Alberta, Canada
<b>Commission date</b>	2011	2007	H2 2013	2013	2013	2018
<b>Plant owner</b>	Qatar Petroleum, Shell	Qatar Petroleum, Sasol	Uzbekneftegaz (UNG), Sasol, Petronas	Chevron Nigeria Limited (75%), NNPC (25%)	Sasol	Sasol Canada
<b>Production capacity</b>	140,000 barrels per day	34,000 barrels per day	38,000 barrels per day	33,000 bpd, rising to 120,000 bpd by 2023	84,000 barrels per day	48,000 rising to 96,000 barrels per day
<b>Products refined</b>	Gasoil, Kerosene, Naphtha, Paraffin	Diesel, Kerosene, Naphtha, LPG	Diesel, Kerosene, Naphtha, LPG	Diesel, Naphtha, LPG	Diesel, Naphtha, LPG	Diesel, Naphtha, LPGs
<b>Cost</b>	~\$18.5 billion	\$950 million	\$4 billion	\$8.4 billion	\$10 billion	\$8 billion

It can be said roughly that Qatar is producing 175,000 barrels per day of GTL, which constitutes as the highest production capacity of GTL in the world. The GTL fuel has not yet replaced the conventional fuels fully but they are currently in use in blended forms. This instills a responsibility on the researchers in Qatar to find out the optimum conditions and characteristics of GTL blended fuels, and to examine their suitability for using in ICEs. The demand of Oil and Gas industry in Qatar is also increasing every day and it is bounded by international regulation for clean

environmental and emissions controls. GTL fuels and their blends can provide the solution to this problem for the local and international Oil and Gas markets, as well as the energy sector.

#### **1.1.5 Scope of Present Work**

Now in the present work, the fundamental combustion characteristics of GTL product blends will be studied, as the said have not been investigated thoroughly and there is a huge gap in the study. Especially the blends of conventional diesel with GTL close to none reported characteristics study. There is a need of conducting proper study for blended fuels employing GTL that could reveal the atomization behavior in various environments, behaviors of different mixtures of blends, emissions behaviors and combustion characteristics. One such fundamental combustion characteristic is the laminar flame speed of the fuel, which is very important in predicting the performance of fuel in a Gas Turbine or and Internal Combustion Engine (ICE). The flame speed depends on many parameters including the fuel composition. A research done previously by Ibrahim and Ahmed [7], concluded that the flame speed of the blended mixture of two fuels is higher than their individual flame speeds at same test conditions. Therefore, there is a need to investigate the flame speed behavior of GTL fuel blended with conventional fuel.

## 1.2 Project Aim and Objectives

Based on the background given in the previous section, the aim of this project is:

*To design, manufacture and run an experimental facility for the measurement of laminar flame speed of liquid fuel blends under different initial temperatures and equivalence ratios in a specially designed state of the art cylindrical bomb test rig.*

The major objectives of this project are given as follows:

- Designing and fabricating a test rig suitable for running the flame speed measurement experiments
- Benchmarking the flame speed measurements of conventional diesel for determining the reliability and accuracy of the designed setup
- Measuring the flame speed of GTL and its 50/50 (by volume) blend with conventional diesel
- Finding out the effect of changing in equivalence ratios and initial temperatures on the flame speeds of tested fuels



### 1.3 Project Methodology

The objectives of this project are to be achieved by following the project methodology shown in Figure 1.

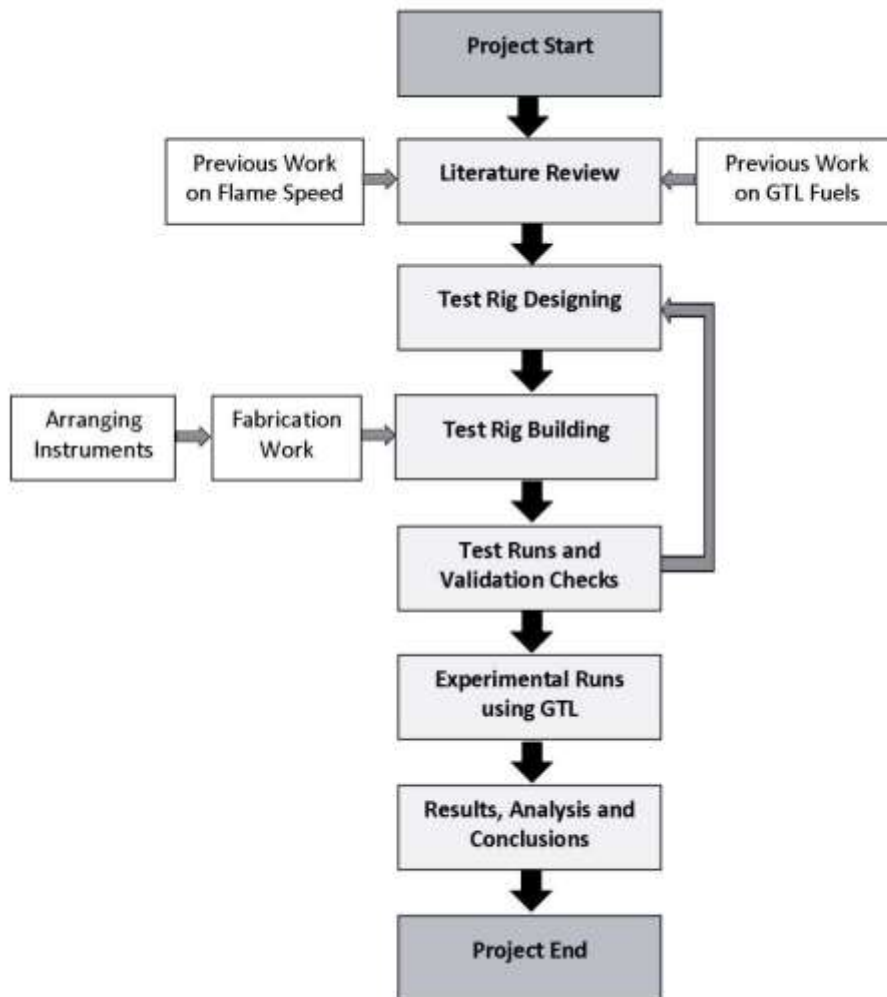


Figure 1 - Project methodology flow chart

The details of the stages of the project show in the methodology flow chart are briefly summarized as follows.

- Conduct a thorough literature review on the topic of flame speed and previous experimental investigations that had been used to measure it
- Design and fabricate the required test rig suitable for running the flame speed measurement experiments, which includes arranging all materials for the fabrication of test rig and selecting appropriate instrumentation and measuring devices
- Cover all the safety issues and risk factors associated with the setup
- Running the test runs and ensure proper functioning of all components and making modifications in the test rig design and settings to achieve desired results
- Benchmarking the flame speed measurements of conventional diesel for determining the reliability and accuracy of the designed setup
- Finding the flame speed of GTL and its blend with conventional diesel at different equivalence ratios and initial temperatures
- Analyzing the results obtained from experiments, compare it with the previous work in literature and discuss the new trends observed
- Project dissemination

The next chapter will discuss the literature review done for this thesis.

## **CHAPTER 2. LITERATURE REVIEW**

This chapter of the thesis will discuss the detailed literature review about the topic suggested in the introduction. The review starts by giving some information about the GTL fuel in detail along with the previous research done on it. Next, the flame speed and different experimental setups for its measurement is discussed. The selected experimental method for this project is studied in depth highlighting the previous research done using that method, along with a brief discussion on their results. After each reviewed investigation, a research gap is identified in its concluding remarks.

### **2.1 Gas-To-Liquid (GTL) as Alternative Fuel**

#### **2.1.1 Introduction to GTL**

Gas to Liquids (GTL) is a recently developed clean alternative fuel which is named after the chemical conversion process. GTL is a technology used to convert a carbon containing raw product, to a wide range of synthetic fuels use in different industries and applications. The raw product can either be a natural gas, coal, or biomass.

GTL production is growing and of special interest in regions where gas reserves are abundant but the sources are remote or where the excess natural gas is flared into the environment. As a consequence of strict regulations imposed on flaring and

natural gas venting, the oil producing countries are now looking into further development of cleaner GTL fuels. Various companies like Shell, Sasol and Chevron are pursuing GTL production technologies and attracting the gas rich countries for setting up GTL production plants to overcome fuel shortage, cleaner fuels and less environmental pollution.

### **2.1.2 GTL Production Process**

The basic technology of the GTL industry dates back to 1923 when two German scientists, Franz Fischer and Hans Tropsch, invented a process called Fischer Tropsch (FT) that could convert natural gas to a hydrocarbon mixture which could then be upgraded into petroleum products. The FT technology provides an alternative to traditional crude oil refining, as liquid petroleum products, most notably diesel fuel, can be produced from a non-liquid input, natural gas. GTL production chain process uses the following three steps process to manufacture its products [8]:

- Formation of syngas
- Conversion of syngas by catalytic synthesis
- Formation of products by cracking

The overall GTL production process is summarized in Figure 2.

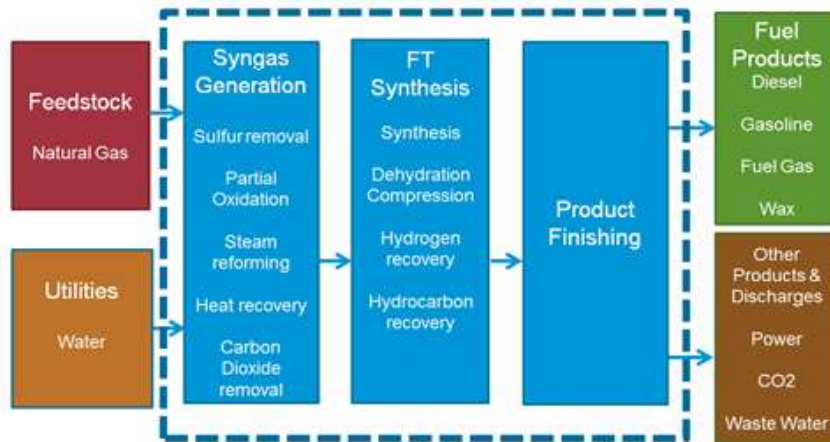


Figure 2 - GTL production process [9]

The first step in the FT process is converting the natural gas (methane) into Syngas, which is a mixture of hydrogen, carbon dioxide, and carbon monoxide. The syngas is further refined to remove water, carbon dioxide and mainly sulfur which prevents the contamination of catalyst. After that, the main process, FT reaction, is carried out to combine hydrogen with carbon monoxide to form different liquid hydrocarbons. These liquid products are then further processed using different refining technologies into products, such as diesel, gasoline, jet fuel, and waxes [9]. Table 2 shows the three main GTL products and their properties that are crucial to the energy industry.

Table 2 - Properties of GTL products [10]

Specifications	GTL diesel	GTL kerosene	GTL naphtha
Density (kg/cc)	0.780	0.738	0.690
Cetane number(CN)	75	58	N/A
Flash point ( °C)	88	42	N/A
Aromatics (vol%)	< 1	< 1	0
Sulfur content	0	0	0
IBP ( °C)	200	155	43
FBP ( °C)	360	190	166
Comparison of GTL product quality specifics vs. standard	Higher CN 75 vs. ~48 (conventional diesel)	Higher smoke point ~110 °C vs. 25 °C (conventional)	Higher paraffins ~100% vs. 50%

The GTL product focused in this thesis is the GTL-diesel, which is offered as a replacement fuel for the conventional diesel. Therefore, a comparison of combustion characteristic like laminar flame speed is required for both fuels and find out how GTL can be adopted as alternative fuel.

### 2.1.3 Previous Research Work on GTL

Previously, there has been many reviews and research investigations, which focused mainly on finding the emissions data and use of GTL fuel in engines as a primary fuel. Some studies compared the engine performance parameters and the exhaust emissions emitted from CI engines fueled by conventional diesel, GTL, and GTL blended with conventional diesel. There is also some work done for studying the mixing of bio-diesel and alcohols with GTL to compare the performance and engine emissions of engines.

Norton *et. al.* [11] investigated the torque and range for a heavy duty truck diesel engine at different speeds and load conditions, using GTL fuel. They reported a decreased in torque with GTL as compared to conventional diesel, with average range about 3% - 8%. Alleman and McCormick [12] in a review paper investigated the GTL properties and exhaust emissions data. They concluded that there is a significant decrease in NO<sub>x</sub> and PM, by 13% and 26% on average compared to conventional diesel. Alleman *et. al.* [13] also investigated the effect of after treatment of exhaust using catalyzed diesel particle filters (CDPF) for engines running with GTL fuel. The results showed that without the CDPF, GTL gave reduced regulated emissions by 58% for HC, 10% for CO, 8% for NO, and 33% for PM when compared with conventional diesel. With the CDPF, the GTL gave even more emissions reduction.

A recent review paper by Sajjad *et. al.* [5], compared about 150 other works related to GTL fuel and its blends with conventional diesel. But all of the previous work is focusing on studying the engine performance parameters and emissions data using GTL fuel. But there has been no research done for finding the flame speed of GTL fuel and its blends with conventional diesel, which is a very important combustion characteristic for any fuel. Therefore, there is a need to find out the proper testing method and find out the flame speed of GTL fuel blends experimentally.

## 2.2 Flame Speed

Flame Speed is a very important fundamental characteristic of a fuel mixture that can give the information about the atomization, reactivity, diffusivity, and exothermicity. The flame speed of a fuel is defined as a physio-chemical constant for predetermined combustion mixture of that fuel and air. Flame speed is the speed at which a one-dimensional plane flame front travels normal to its surface, relative to unburnt mixture [14].

The precise determination of flame speed is essential for gas turbine combustors, design engines, turbulent combustion simulations and validation of chemical kinetic mechanisms. Moreover, the explosion protection systems, military bombs and pressure vessel calculations depend on the accurate measurement of flame speed.

There are two types of flame speeds: laminar and turbulent. The laminar flame speed is calculated at steady state, while the turbulent flame speed is calculated when there is turbulence in the mixture [15].

The laminar flame speed can also be used to model turbulent flame speed when the mixture is not steady [16]. A previous research conducted by Klimov [17], studied the relation between the laminar and turbulent and gave the following equation:

$$\frac{S_T}{S} \sim \left[ \frac{S_N}{S} \right]^0 \quad \text{Eq. 1}$$



Here in equation 1,  $S_T$  is the turbulent velocity,  $S_N$  is the laminar velocity.

## 2.3 Test Rigs for Flame Speed Measurements

There have been many experimental test rigs designed and techniques developed for the measurement of flame speed of a fuel air mixture. All have different advantages and disadvantages. This section of the thesis will discuss some of these flame speed measurement setups taken from the previous research work.

Andrews and Bradly [18], has done a critical review about the effectiveness and shortcomings of many of these experimental techniques and test rigs. They have divided these test rigs into two types:

- Constant Pressure
  - Example: Slot Burner Method
  - Example: Bunsen Burner Method
- Constant Volume
  - Example: Spherical Bomb Method
  - Example: Soap Bubble Method

This classification is based on the ability of test rig to accommodate various ranges of pressure and temperature conditions for the tests. The constant pressure methods are conducted mostly at the atmospheric pressure and constant

temperature. On the other hand, the constant volume methods can be conducted at a variety of initial temperatures and initial pressures [19].

In this project, the bomb method is taken as the desired test rig for the measurement of GTL fuel blends at various equivalence ratios. The justification for this is given in the next section of the thesis.

### 2.3.1 Slot Burner Method

The slot burner method employs a pipe with a rectangular slot cut into it along the length of its surface. The air-fuel mixture is made to flow inside the pipe to create a flat velocity profile. This causes the flame to exit the slot in a triangular shape, as shown in the Figure 3 [20].

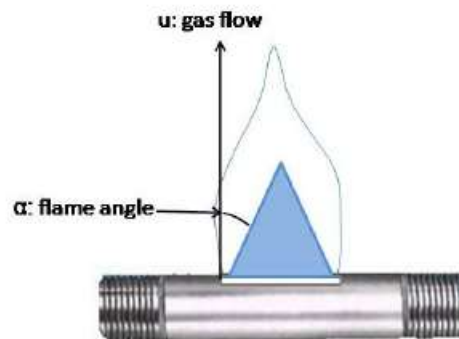


Figure 3 - Slot burner method [20]

The angle of the flame normal to the slot surface is used to calculate the flame speed of the mixture. The formula is given as:

$$S_U = U \sin \alpha \quad \text{Eq. 2}$$

Here  $S_U$  is the flame speed (cm/s),  $U$  is the flow of air-fuel mixture (cm/s) and  $\alpha$  is the oblique angle normal to the gas coming out of slot [21].

The disadvantage of this method is that it is very difficult to measure the angle  $\alpha$  because the flame can get turbulent and disturbed as it moves out of the slot into the atmospheric conditions. This can cause the flame to come out in curved fashion that will give error in calculating the angle.

### **2.3.2 Bunsen Burner Method**

This is the simplest of all the methods for calculating the laminar flame speed. In this method, the air-fuel mixture is moved in a vertical pipe at a certain flow rate and the mixture is ignited. The surface area of the flame coming out of the top open end of the pipe is then divided by the air-fuel mixture burnt per second [22].

Figure 4 shows a typical Bunsen burner method setup:

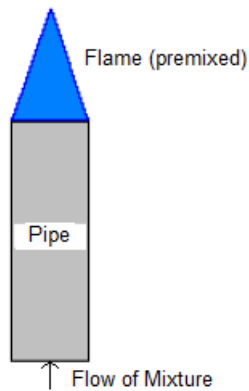


Figure 4 - Bunsen burner method [22]

The formula for calculation of flame speed (S) is given as:

$$S = \frac{\text{input volumetric flow}}{\text{total flame area}} \quad \text{Eq. 3}$$

This is the general concept of this method and there are many techniques for performing this experiment; such as angle method with Schlieren cone, particle track method, and Frustrum Method. However, Vagelopoulox and Egolfopoulos established that there is huge uncertainty as to which technique of Bunsen burner is most correct [23].

The advantage of this method is that it is fairly simple and easy to setup. But the disadvantages overcome the advantages as this method is not accurate, doesn't have significant theoretical reliability, and is not suitable for high speed flames.

### 2.3.3 Tube Propagation Method

Another method for flame speed measurement is the tube propagation methods. Again there could be many setups for this method like vertical tube, horizontal tube etc. Almarcha, Denet and Quinard have conducted a similar experiment by using a vertical 1.5 m long tube [24]. In this method, a vertical pyrex tube is filled with a controlled air-fuel mixture from one side while the other side is kept open. The mixture is ignited at one end and snapshots of flame propagation were taken by a high speed camera. This setup is shown in Figure 5.

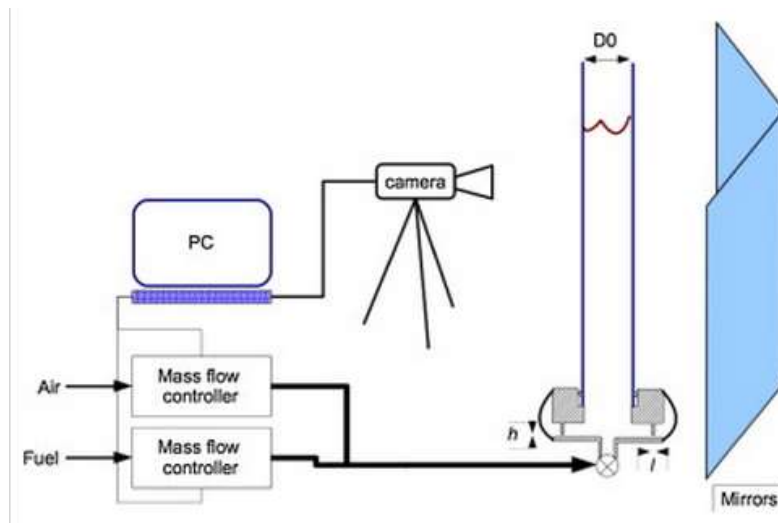


Figure 5 - Tube propagation method [24]

The flame speed is calculated by the help of frame/sec of the high speed camera. Also, the same can be calculated by using two thermocouples or pressure sensors installed at a distance that can give an indication of distance cover in certain time.

A disadvantage of this method is that the effect of walls cooling of the tube can give error in the readings, and only the average flame speed can be measure with this method.

#### 2.3.4 Soap Bubble Method

The soap bubble method for measurement of flame speed is a relatively simple method and the combustion takes place at constant temperature. In this method, a soap bubble is formed by blowing the air-fuel mixture into it. This mixture is then ignited by using spark circuitry and the flame starts to propagate outwardly in a spherical fashion [25]. The soap bubble method is shown in Figure 6.

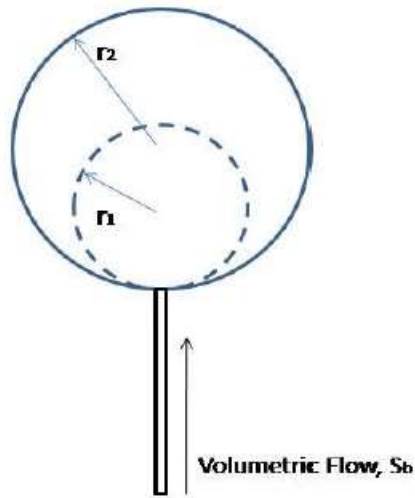


Figure 6 - Soap bubble method [25]

All this activity is recorded by using high speed camera and the initial and final diameters of the soap bubble are measure to get the flame speed. The following

formula is used:

$$S_U = \left(\frac{r_1}{r_2}\right)^3 S_b \quad \text{Eq. 4}$$

Here  $S_U$  is the flame speed (cm/s),  $S_b$  is the volume flow (cm<sup>3</sup>/s), and  $r_1$  is the initial while  $r_2$  is the final radius of the soap bubble (cm) [21].

A disadvantage of this method is that air-fuel mixture can diffuse with the soap bubble and some of the water can get mixed with the initial mixture. To avoid the disturbance of flame spherical shape by convection, the flame needs to be at high speed. Also, sometimes the flame cannot have the spherical shape and it gets very difficult to measure the final diameter of the flame.

### **2.3.5 Constant Volume Bomb Method**

The constant volume bomb method works similar to the principles of soap bubble method. It can have a spherical bomb or cylindrical bomb construction. In this method, a quiescent combustible mixture is injected in the bomb and ignited at the center using electrodes. As the flame in progress, the expansion of the burned gases in a rigid volume causes both pressure and temperature of the unburned gas to increase due to adiabatic compression. A rising pressure rise signal or photography of the expanding flame is recorded and analyzed using different calculation models.

The advantage of this method is that it uses less amount of fuel, and give good

control over initial conditions of the mixture. A drawback of this method is the non-adiabatic conditions at the bomb walls, which can be solved by using a fast data acquisition system (DAQ).

There has been several test rig configurations used in the past for the measurement of flame speed by bomb method. Some of these test rigs along with their calculation formulas and findings will be discussed in detail in the next section, as it is very similar to the method employed in this project.

## **2.4 Previous Research Work using Bomb Method**

Previously, a research work had been done by Huzayyin *et. al*, [26] for the measurement of laminar flame speed of LPG-air and Propane-Air mixtures using a combustion bomb. They used a closed cylindrical chamber made up of thick steel that can hold an internal pressure of up to 90 MPa. The end covers of the cylinder has a 30mm diameter quartz glass window as a viewing port. The bomb has many ports for injecting air-fuel mixture, gas exhaust, pressure transducer pickup, and spark ignition circuit. The following schematic in Figure 7 shows the arrangement of this flame speed measurement method.



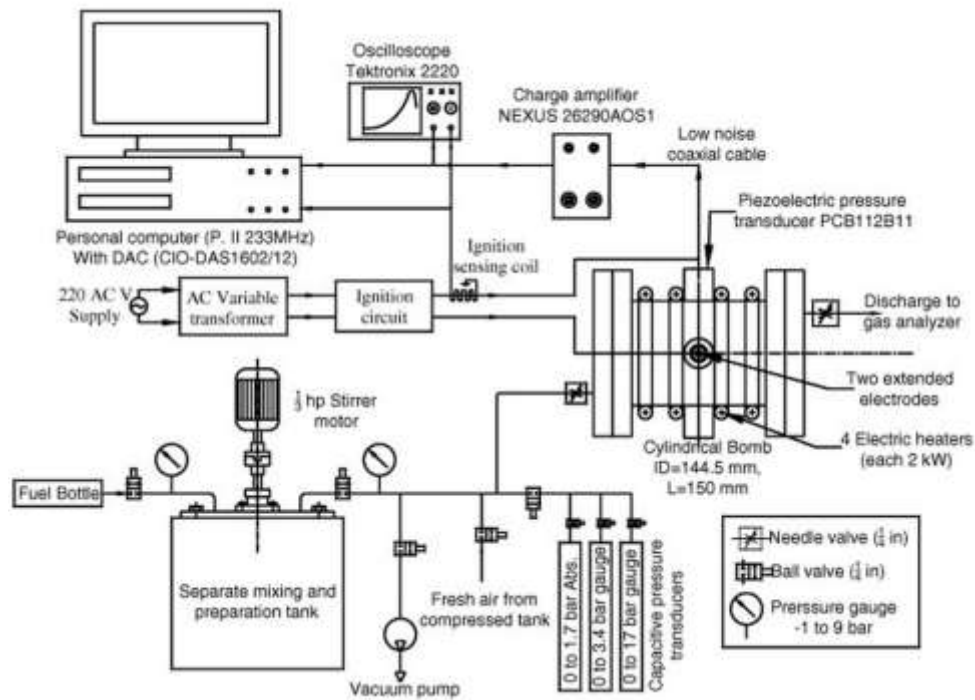


Figure 7 - Spherical bomb method schematic [26]

As seen in Figure 7, the air-fuel mixture is prepared in a separate mixing tank that has an electric motor stirrer for uniform mixing, while the cylindrical bomb is kept at a predetermined temperature using external electric heaters. Before injecting the fuel, the bomb is scavenged by using a vacuum pump and the vacuum is maintained at 2.5 kPa. The mixture is then introduced in the bomb and kept in there for about 3 minutes to reach a steady state. Then this mixture is ignited by using two stainless steel electrodes extended inside the bomb having spark gap of 0.8mm connected to the capacitive ignition coil circuit. At the time of combustion, an oscilloscope attached with pressure transducer is used to measure the pressure versus time signal and this data is then saved in digital form using Data Acquisition System (DAC).

This pressure signal is used to calculate the flame speed of the mixture, and there is no provision for flame speed imaging. Also, the mixture in this method is prepared outside the bomb in a separate mixing tank. The results for this study investigated the effect of change in equivalence ration on the flame speed of different mixtures of gases.

Another similar research work, done by Bradley and Mitcheson [27], concluded that a universal equation can be used to find the flame speed in relation to pressure increase (dP). This equation is given as:

$$\frac{dP}{dt} = \frac{3S_L \rho_u}{R_S \rho_i} (P_e - P_i) \left[ 1 - \left( \frac{P_i}{P} \right)^{\frac{1}{\gamma_u}} \left\{ \frac{P_e - P}{P_e} - P_i \right\} \right]^{\frac{2}{3}} \quad \text{Eq. 5}$$

Here,  $\rho_u$  is the density unburnt mixture

$\gamma_u$  is the specific heat ratio of unburned mixture

P is the pressure at the time of combustion

$P_e$  is the equilibrium pressure

$P_i$  is the initial pressure

A disadvantage of the spherical bomb method mentioned in the literature is that the pressure measured by this technique is inconsistent. This problem has been solved by using several other numerical models employing pressure data for the calculation of flame speed. These models are briefly summarized in Table 3.

Table 3 - Numerical models for flame speed

Reference	Model
Dahoe et al. [27]	$X = \frac{P - P_i}{P_c - P_i}, \quad r_b = r \left( 1 - \frac{P_i T_u P_c - P}{P T_i P_c - P_i} \right)^{1/3}$ $S_L = \frac{r}{3} \left( \frac{P_i}{P} \right)^{\frac{1}{3}} \frac{1}{(P_c - P_i)} \left[ 1 - \left( \frac{P_i}{P} \right)^{\frac{1}{3}} \left( \frac{P_c - P}{P_c - P_i} \right) \right]^{-\frac{1}{3}} \frac{dP}{dt}$
Rallis et al. [28]	$\bar{\beta} = (P/P_i)^{\frac{1}{\gamma_u}}, \quad \bar{\alpha} = \frac{m_b T_c P}{m_c T_b P_c}, \quad r_b = r \left( \frac{\beta - 1}{\beta - \bar{\alpha}} \right)^{\frac{1}{2}}, \quad PR = \frac{P}{P_i}$ $X = \bar{\alpha} \left( \frac{\beta - 1}{\beta - \bar{\alpha}} \right), \quad S_L = \bar{\alpha} \left[ \frac{dr_b}{dt} + \frac{r_b}{3\bar{\alpha}} \left( \frac{\gamma_u - 1}{\gamma_u} \right) \left( \frac{1 - \bar{\alpha}}{\beta - \bar{\alpha}} \right) \frac{dP}{dt} \right]$
Babkin and Kononenko [29]	$E_i = \frac{M_i T_{bi}}{M_b T_i}, \quad X = \frac{\bar{\beta} + \frac{2\gamma_u - 1}{\gamma_u - 1} (1 - \bar{\beta}^{1-\gamma_u}) - 1}{G}, \quad r_b = r(X\bar{\alpha})^{\frac{1}{2}}$ $G = \gamma_b \left[ E_i - \frac{\gamma_u}{\gamma_b} \frac{\gamma_b - 1}{\gamma_u - 1} \right] \bar{\beta}^{1-\gamma_u} + \frac{\gamma_b - \gamma_u}{\gamma_u - 1}, \quad \frac{d\bar{\beta}}{dt} = \frac{\bar{\beta}^{\frac{\gamma_u - 1}{\gamma_u}}}{\gamma_u P_i} \frac{dP}{dt}$ $S_L = \frac{r}{3G} \left( \frac{\bar{\beta} + X - 1}{\bar{\beta}} \right)^{\frac{1}{2}} \left( \gamma_u + \frac{\gamma_b(1 - X)}{\bar{\beta} + X - 1} \right) \frac{1}{\bar{\beta}} \frac{d\bar{\beta}}{dt}$
Metghalchi and Keck [30]	$x \cong \frac{P_i v_i}{\gamma_f (R_f T_f - R_u T_u)} \left[ \frac{P}{P_i} - 1 - \left( \frac{\gamma_u - \gamma_f}{\gamma_u - 1} \right) \left( \left( \frac{P}{P_i} \right)^{\frac{\gamma_u - 1}{\gamma_u}} - 1 \right) \right]$ $\frac{dx}{dP} = v_i \left[ 1 - (1 - x) \frac{v_u}{v_i} \left( 1 - \frac{\gamma_b}{\gamma_u} \right) + a_\eta + a_b + a_w \right] / [\gamma_b (R_b T_b - R_u T_u)]$ $r_b = r \sqrt{X \left( \frac{P_i}{P} \right)^{\frac{1}{\gamma_u}}}, \quad S_L = \left( \frac{P_i}{P} \right)^{\frac{1}{\gamma_u}} \frac{r^{\frac{1}{2}}}{3r_b^{\frac{1}{2}}} \frac{dx}{dP} \frac{dP}{dt}$

The above mentioned research used all of these models by using Engineering Equation Solver (EES) to find the numerical solutions for the measurement of flame speed.

Another research conducted using similar test rig is by Bradley *et. al*, where they used a spherical steel bomb, called Mk2 Combustion Bomb (Figure 8), with 150 mm diameter glass windows for measuring the laminar flame characteristics of ethanol and air mixtures [32].



*Figure 8 - Mk2 combustion bomb at University of Leeds*

The same test rig has also previously been used by Bradly *et. al.*, for the measurement of flame speed for iso-octane blends [33]. This experiment was conducted by heating the bomb to 395 K by a 6000 Watts electric heater. There were four electric motor fans installed directly to the bomb for proper mixing of the mixture. Also the fans can facilitate the mixture in evaporating completely because this will increase the heat transfer from the coils. The amount of ethanol to be injected in bomb was calculated by the stoichiometric calculations, because the volume of bomb is known. A syringe and needle valve is used to inject the fuel inside the bomb. The mixture was ignited by using automotive ignition coil spark system. The pressure map was recorded using a pressure transducer and flame images were taken by schlieren cine photography. The flame radius obtained from high speed imaging were plotted against time to get the flame speed.

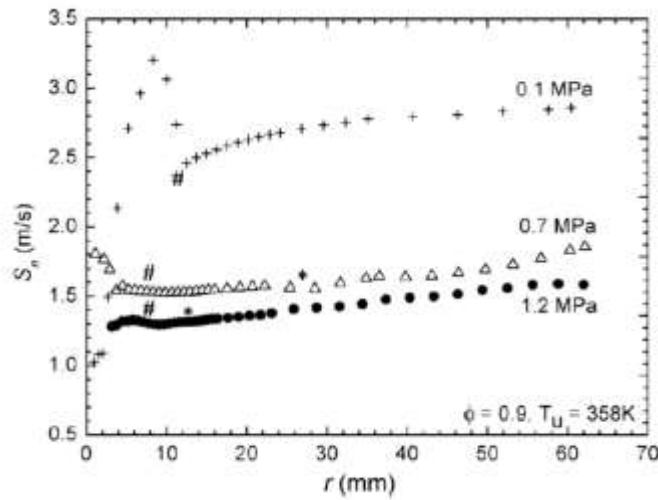


Figure 9 - Plot of flame speed vs. flame radius [32]

Figure 9 shows that the flame speed ( $S_N$ ) varies with the radius. This plot shows that the variation is quite small. Also the average error in calculating [34] the flame speed by this method in Bradley's experiment was 1.4%.

Another research work done by Radwan, *et. al.* [35], used a cylindrical bomb method to investigate the laminar flame speed of Jojoba Methyl Ester in comparison with conventional diesel. This research is also closely related to present study as it is comparing an alternative fuel with conventional diesel. The experimental setup for this research is shown in Figure 10.

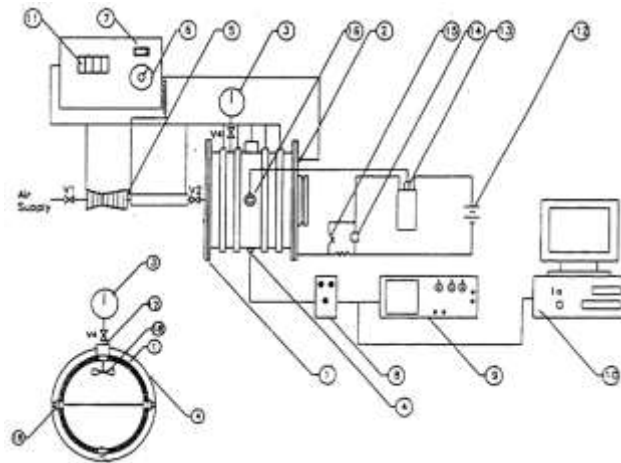


Figure 10 - Cylindrical bomb test rig by Radwan

This test rig also used a steel bomb construction with a separate mixing tank for the mixture preparation. The bomb is equipped with heaters, thermocouples and a pressure transducer. There is no optical glass window in this tests rig and the flame speed can be calculated by relying on the pressure signal only. The calculation model, suggested by Lewis and Von Elbe [36], is used for getting the flame speed from the pressure and time data. This is a fairly simple model to calculate the flame speed as compared to the more complex models mentioned earlier.

The results of this experimental work studies the effect of change in equivalence ratio and initial temperature on the laminar flame speed of fuels, as shown in Figure 11.

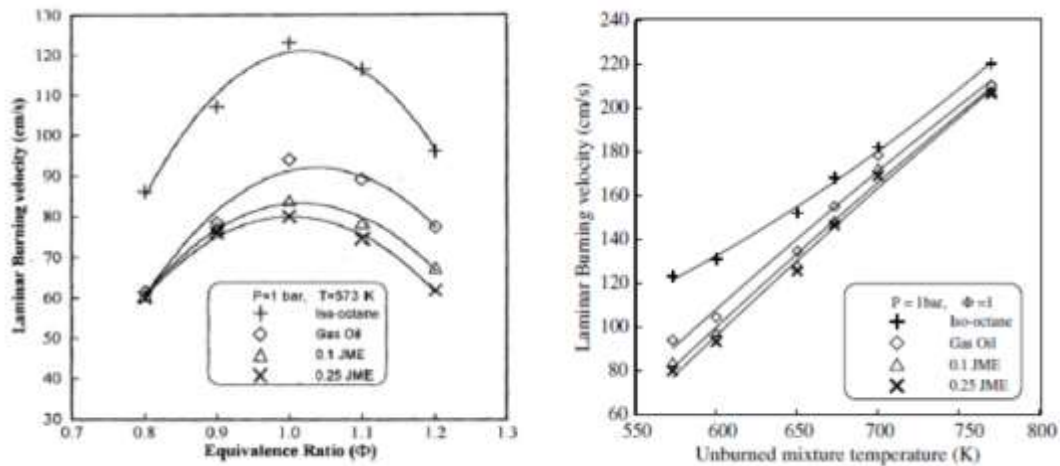


Figure 11 - Results of experimental study by Radwan

The results for the experimental work by Radwan, *et. al.*, showed that the flame speed is low at lean and rich side of the combustion mixture, while it is highest at the stoichiometric conditions (i.e.  $\Phi=1.0$ ). Also, the flame speed is found to be increasing with the increase in initial temperature of the mixture. The research work also compare the effect of initial pressure of the mixture on the flame speed but this was not under the scope of the present work.

All the experimental methods, discussed above were found to be attractive to the given objectives of this thesis. Many of the test rig design features mentioned in the literature are similar to the proposed test rig. Also, the results obtained in these studies are also the desired target results for this study. Therefore, the next section will discuss the selected experimental method in detail and various test rig design features and modifications are also highlighted.

## **CHAPTER 3. TEST RIG DESIGNING & FABRICATION**

This chapter of the thesis will discuss in detail all the steps involved in the designing and fabrication of the selected test rig setup. The chapter starts by explaining the key features of the proposed experimental method and setup. The selected design went through many design and fabrication modifications before coming in the final shape, which is explained in the last section of this chapter.

### **3.1 Proposed Experimental Method**

As mentioned in literature review, the proposed experimental method in this project is the cylindrical bomb method. The project aims to design, manufacture and run an experimental facility for the measurement of laminar and turbulent flame speed of liquid fuels under different initial temperatures and equivalence ratios in a specially designed state of the art spherical bomb test rig. Studying the designs from the previous studies, a schematic layout as shown in Figure 12, of the proposed experimental design setup was drawn which includes the key features from various experimental setups and is also fulfilling the goals of this project.



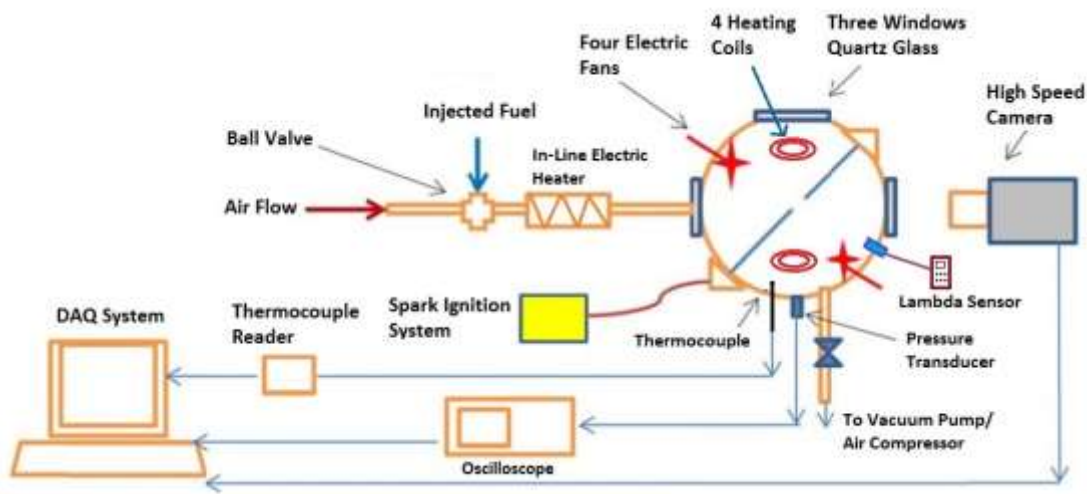


Figure 12 - Schematic of proposed test rig

The proposed test rig consists of a cylindrical combustion bomb with four internal temperature controlled heating coils. The bomb will be equipped with three orthogonal quartz glass windows, three ports, four stirrer fans, two central stainless steel electrodes for generating the spark, pressure transducer, lambda ( $O_2$ ) sensor and thermocouples. The test rig also includes air supply system, vacuum system, and spark ignition system. The pressure transducer will be connected to an oscilloscope and a data acquisition system.

The air compressor will be used to charge a calculated amount of air inside the bomb, while the vacuum pump will be used to evacuate the bomb before and after experiment. Also, the air-fuel supply line will be wrapped with electric heating wires to ensure that no fuel condensation takes place during injection. A four internal electric heaters will be used to maintain the temperature inside the bomb, which

can be monitored by the K type thermocouples. The four electric fans will be used to ensure proper fuel-air mixing and getting a homogenous mixture obtained inside the bomb. For laminar flame speed measurements, the fans can be switched-off and the mixture can be left for 2-5 minutes to reach equilibrium state. The test rig can also be used for turbulent flame speed measurements by adjusting the four fans to the desired speed to produce the required turbulent intensity (but this is not in the scope of this project). The air-fuel mixture and the equivalence ratio can be confirmed by the lambda sensor connected to the bomb.

After all initial readings, the air-fuel mixture will be ignited by using central electrodes which will be connected to spark ignition coil circuit. The pressure rise signal after igniting the mixture will be detected by the pressure transducer for further analysis to calculate the burning velocity. Also the flame propagation can also be recorded by using a high speed camera by capturing the flame front through one of the quartz windows.

The acquired data from pressure sensor, thermocouple, lambda sensor and high speed camera can be used to find out the flame speed of the test fuel mixture using one of the methods mentioned in the literature review.

## 3.2 Cylindrical Bomb Test Rig Designing and Manufacturing

This test rig was design and built in two phases. Phase one was the initial design and fabrication of test rig based on the proposed system. Phase two was the modifications done in the design after finding out certain issues with the proposed design. The whole process of designing and fabrication of test rig took around two years to complete. The next sections of the thesis briefly highlights phase one of the designing and manufacturing steps of the proposed cylindrical bomb test rig.

### 3.2.1 Design and Fabrication Process – Phase One

After thorough research and discussing with industry experts, a cylindrical bomb was designed to be made up of a steel shell of 400 mm internal diameter, 5mm thickness and a length of 650 mm. The two sides of this shell are closed by flanges bolted onto the drum by eight 17 mm hexagonal bolts, as shown in Figure 13.

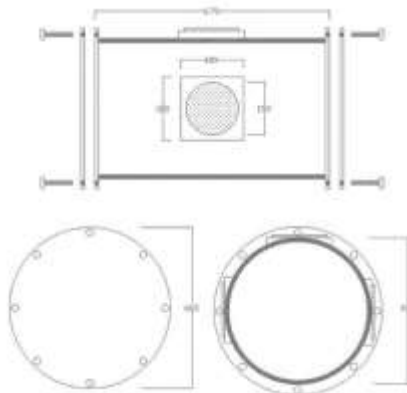


Figure 13 - Sketch of bomb shell, flanges and windows sketch

The above shown sketches were given to a local company, Al-Mannai Corporation, for the manufacturing of the bomb. A four leg support stand was also built to hold the bomb in desired position, as shown in Figure 14.



*Figure 14 - Bomb and stand manufacturing*

Along the circumference of the bomb, three windows were installed that were 150 mm in diameter each and were equipped with quartz glass for visualization. The windows were at 90 degrees angle to each other and can be used to high speed imaging and laser techniques. Also, three ½" steel pipes with gate valves were welded on the bomb to provide ports for vacuum pump, exhaust and air-fuel injection. This is shown in Figure 15.



*Figure 15 - Windows and ports installation*

In addition, along the center of circumference of bomb, four stirrer motors were mounted and a custom made fan was installed on the shaft of the motor inside the chamber, as shown in Figure 16.



*Figure 16 - Fans design and installation*

The fans were also mounted at 90 degrees angle from each other. Also it was made sure that the fans were facing the central point of the bomb where the spark is going

to ignite. The blades of the fan were bent at 60 degrees angle to ensure proper mixing of the mixture and adequate turbulence intensities. For fan shaft sealing, a novel design was introduced as shown in Figure 17.

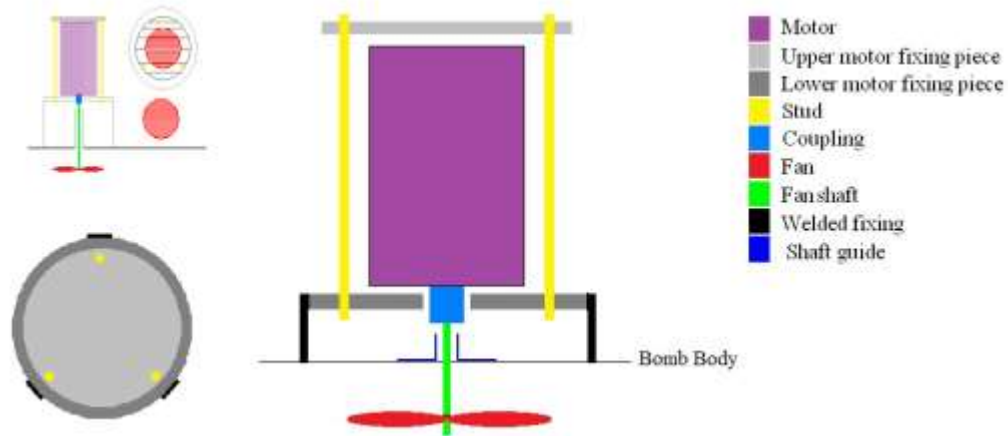


Figure 17 - Fan shaft sealing design

The design was tested to ensure that there is no air leakage from the shaft area of the fans. The wiring for the fans was done by using two dimmer switches to control fans speed.

After installing the fans, the next step is to install the spark electrodes and spark coil system. The two electrodes, 3 mm diameter each, were inserted in the bomb and fixed from the side flanges at the center so that the ends of two electrodes meet in the center of the bomb in front of the glass window, as shown in Figure 18.



*Figure 18 - Spark electrode system [34]*

A gap of 2 mm was kept between the electrodes and the ends were sharpened down to 1 mm to reduce any energy loss from the spark. A 12V DC automotive spark ignition coil was also placed with the test rig but was not installed.

### **3.2.2 Pending Works on Test Rig for Phase Two**

The following accessories arranged in phase one but not installed:

- An automotive 12 volts ignition coil circuit and its push button
- Two 3 mm stainless steel electrodes
- Heating coils and their thermostat controllers
- K Type thermocouples
- Vacuum pump
- Pressure transducer and Oscilloscope/DAQ
- Lambda (Oxygen) sensor

It can be seen that phase one only cover the test rig manufacturing and arrangement of materials. There is still a lot of work needs to be done in order to make this test rig fully functional. Therefore, the next section of the thesis will discuss further developments and modifications done in phase two.

### **3.3 Test Rig Developments and Modifications – Phase Two**

This section of the thesis will discuss the steps involved in further designing, developments, improvements and modifications in the test rig received after manufacturing in phase one. There have been many trials and errors in the development of the test rig. Many challenges were faced in terms of right parts selection, insulation material, electrical wiring, heating system and overall safety of the test rig. All these design and manufacturing stages will be highlighted in the next sections of the thesis.

#### **3.3.1 Installation of Control Boards and Components**

The combustion bomb used for the purpose of this project has a main switch, temperature controllers, switches and other devices that needs to be fixed in one place. So, the bomb stand needs to be fixed with a control board. Therefore, two control boards were made up of transparent plastic sheets and installed on both sides of the test rig support stand, as shown in Figure 19.





*Figure 19 - Control board components installation*

The following components were installed on the control boards:

- Two thermostat boxes
- Two fan switches
- Main circuit breaker switch
- Current controller for thermostat

The next job was the electrical termination of the control board components. For this, the main circuit breaker switch was connected with AC mains. From the main circuit breaker, the power was given to the two thermostat controls which will be connected to the heating coils later on. After the electrical termination, all the wiring, connectors, joints and fuses were double checked to ensure safety. The power was switched on and all the components were tested to have proper working.

### 3.3.2 Spark Coil Ignition System Installation

The spark coil ignition system was developed in two trials. The first system used a 12V car battery while the second system used AC mains. The second system was found to be more effective after finding out several issues with the DC battery system, like; charging of battery and inconsistency spark. Therefore the idea of using car battery was dropped and second system was developed that used AC mains for current supply. The new spark ignition system consisted of an automotive spark coil, high tension cables, capacitor and a dimmer switch, as shown in Figure 20.

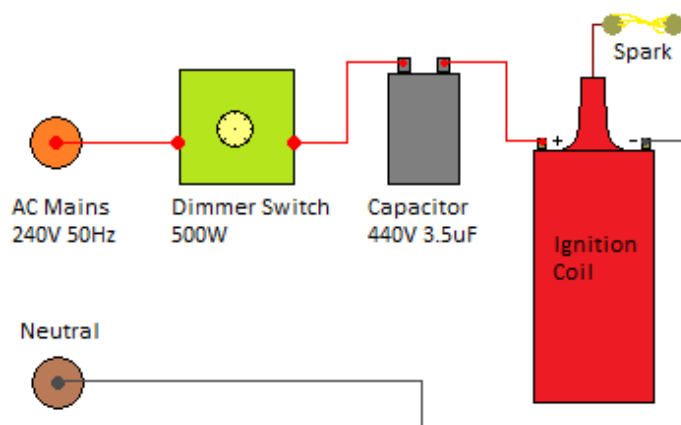
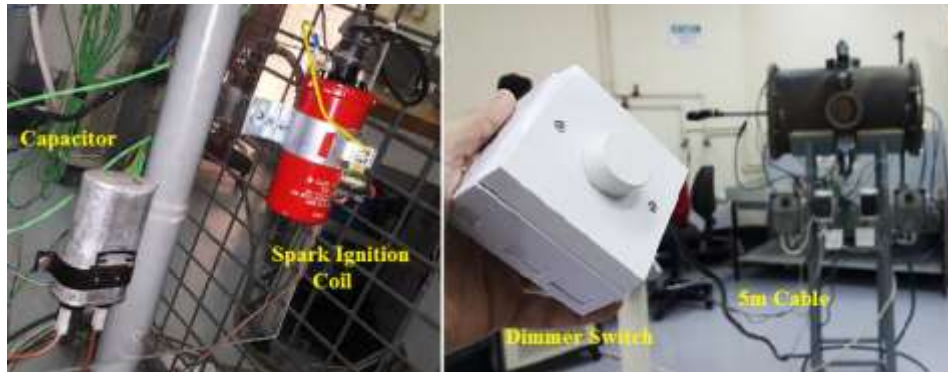


Figure 20 - Spark ignition system diagram

In this system, a 500W dimmer switch was connected to AC mains on one side and to a 440V, 3.5µF capacitor on the other side. The positive terminal of ignition coil was connected with the capacitor and the negative terminal was grounded and connect to neutral. Also, high tension cables were used and attached with the two

stainless electrodes with a gap to 2mm in between them. The ignition system components installed with the test rig are shown in Figure 21.



*Figure 21 - Spark ignition system components*

As seen in the figures, the dimmer switch was attached with a 5m extension cable to operate the spark ignition system from a distance. This will ensure added safety for the operator. Then a spark generated by this system is shown in Figure 22.



*Figure 22 - Spark between two electrodes*

This spark produced is about 20 kV voltage and 200 mA current, which is enough to ignite the flammable mixture at any conditions under investigation.

### 3.3.3 Pressure Transducer Components and Installation

There were two pressure transducers installed on the test rig. This is because the first pressure transducer (Omega) got damaged during the experimentation. Therefore a new one was ordered that was a different model (PCB) but with similar specifications. Both the pressure transducers came with a testing and calibration certificates which showed the relationship between the output voltage and pressure. These certificates are given in Appendix C.

First, a proper mounting place has to be decided for the pressure transducer. The best installation position was decided to be the center circumference of the test rig. In this way, the pressure pick up is closest to the spark origin. After marking the mounting location and drilling a hole through it, internal threads were tapped in that location using tapping tools. Also, a custom adapter (union) fitting was fabricated at the Qatar University mechanical workshop, as shown in Figure 23.



*Figure 23 - Taping hole and machined adapter*

One side of the adapter was bolted on to the test rig, while the other side was bolted to the pressure transducer. The pressure transducer was mounted on adapter using pipe thread Teflon tape for better sealing, as shown in Figure 24.



*Figure 24 - Pressure transducer mounting*

The first pressure transducer selected for this test rig was Omega - Very High Accuracy Amplified Voltage Output Transducer. It has 0 to 5 Bar range with 3m output Cable. The cable had six colored wires; two wires for Input Excitation which was connected with 24V DC power supply; two wires for output voltage which were connected to the oscilloscope; and the last two shunt wires for calibration purposes. The 24V DC power supply for excitation was arranged from the local market. After the connection with power supply and oscilloscope, the pressure transducer was taken off from the test rig and manually tested. The signal was received on the oscilloscope which indicated proper functioning of the pressure transducer as shown in Figure 25.



*Figure 25 - Omega pressure transducer testing*

The Omega pressure transducer got damaged during the first set of experimental runs as the test rig has been transported in and out of the laboratory several times for safety requirements at the University.

The second pressure transducer selected was the Charge Output Pressure Sensor (Model 116B03) from PCB Piezotronics, having a range of 7 bar and an operating temperature up to 343°C. The output pressure response from this sensor is 10 pC/psi, which is then converted by an In-Line Charge Converter (Model 422E35) also from PCB Piezotronics. The inline charge amplifier converts the signal with a gain of 0.99 mV/pC. Therefore, the final calibration factor used for converting the transducer signal to pressure was 6.238 mV/psi. Figure 26 shows both the pressure sensor and the charge converter.



Figure 26 - PCB pressure transducer and PCB charge converter

The PCB sensor was connected to the test rig in the similar way as the Omega sensor using a custom adapter fittings. But the connection with the oscilloscope was slightly different as shown in Figure 27.



Figure 27 - PCB pressure sensor setup

In the new setup, there is additional low noise cable between the charge converter and the pressure sensor. Also, there is a signal conditioner for reducing the noise in the signal. This pressure sensor was also tested manually for its proper working and the signal was successfully received at the oscilloscope.

The selected oscilloscope for this project was the GW-Instek (Model GDS-3152) Digital Storage Oscilloscope with a sampling rate of 150 MHz, as shown in Figure 28.



*Figure 28 - GW-Instek oscilloscope*

The oscilloscope has a function to save the screenshots of the plots, as well as the sampling data in the form of Excel file, which can be used for further analysis. The oscilloscope can also be linked directly to the computer for ease of data retrieval.

### **3.3.4 Installation of Heating Coils**

In order for liquid fuel to vaporize in the combustion bomb, the bomb needs to be kept at approximately 160°C to 300°C. This ambient temperature is supposed to be achieved by installing heating coils inside the bomb for reaching high temperatures in less time. Firstly, only two coils were installed but they were found insufficient for reaching desired temperature. Therefore, four 8" diameter surface heating coils in circular pattern were arranged with load rating of 220 volts and 2100 Watts each.



The two side covers of the bomb were taken removed and the two coils were installed on each cover in upright position, as shown in Figure 29.

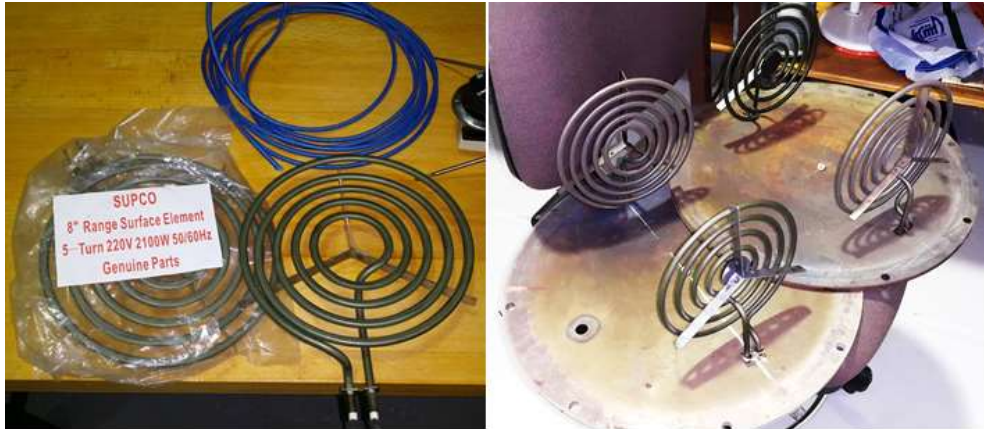


*Figure 29 - Four heating coils*

The two covers were then again assembled with the test rig so that the coils are aligned opposite and symmetric to each other. After that, the wiring from the new heating coils was done using fire proof cables to ensure safety and the coils were tested for proper operation, as shown in Figure 30.



*Figure 30 - Installation of heating coils*

The main AC power was connected to the temperature controller thermostats to ensure that the heating coils automatically turn off after reaching a set temperature and maintain the bomb at that temperature. The test rig was made ready for maximum temperature test discussed in next chapter of the thesis. The temperature reached with the circular heating coils was 300°C in 30 minutes. Also, the temperature was allowed to go beyond 300°C and it was found that the test rig was capable of reaching up to 400°C. The thermostats were set to limit the maximum temperature to 320°C for safety purposes.

It is important to highlight some detail about the thermocouple used for measuring the temperature, which is the type-K thermocouple. The temperature range was from -270 to 1260°C and the melting point was 1400°C. So this was the suitable thermocouple for this project as we are not exceeding more than 350°C. The

accuracy for this was around  $\pm 2.2\%$ . In addition, the thermocouple was connected with a temperature reader module from Omega having option to display two channels as shown in Figure 30 given earlier. It should be noted that the thermocouple has been installed on the cylinder wall to measure the temperature as close as possible to the ignition location.

### 3.3.5 Vacuum Pump and Compressor Installation

The vacuum pump arranged was Marathon Electric vacuum pump. A hose with adapter fitting was assembled with the test rig. Also a flexible wire, terminal connector and 3 pin single phase plug were arranged for electrical termination of vacuum pump, as shown in Figure 31.



*Figure 31 - Vacuum pump connection*

Finally, the vacuum pump was tested by applying suction to the bomb. The pressure dropped to 0.8 Bar which indicated proper functioning of the vacuum pump.

The compressor was also attached with the same outlet of the bomb using another type of fitting. The compressor use was a general purpose air compressor already available in the laboratory, as shown in Figure 32.

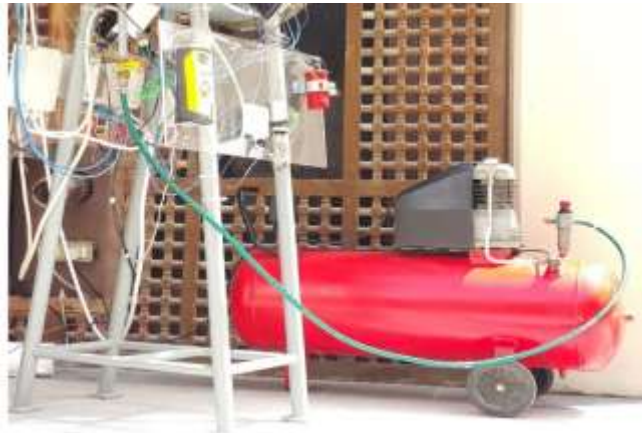


*Figure 32 - Air Compressor*

The compressor can be used for flushing the bomb after each experiment, as well as charging the bomb with the fresh mixture of fuel and air. Also it can be useful for testing the bomb for any leakage.

### **3.3.6 Lambda Sensor Installation**

The lambda sensor used for this experiment was the IMR (Model IMR 1000). This was a hand held unit capable of measuring O<sub>2</sub> percentage (0-21%) with an accuracy of +/- 0.2%. It was also capable of measuring several other gases as well as the temperature. A 6mm copper tubing along with a gate valve were arranged for sampling purposes. On one end, the copper tubing was installed at the center

circumference of the bomb in order to get accurate O<sub>2</sub> percentage near the spark area, while the other end of the copper tubing was connected to the inlet of lambda sensor pump, as shown in Figure 33.



*Figure 33 - Lambda sensor piping and connection*

The lambda sensor with sampling tube was tested by making a small fire in the test rig and checking O<sub>2</sub> percentage, which showed correct working. It is important to mention here that the sensor gate valve should be closed while operating the vacuum pump. Otherwise, it can damage the lambda sensor sampling suction pump.

### **3.3.7 Safety Concerns and Modifications to the Test Rig**

After successfully designing the test rig, it was evaluated by the Qatar University Safety Department. The following three comments and recommendations were received from the safety department:

- To enclose the test rig in a fixed steel cage enclosure

- To install higher capacity exhaust fume hoods in the testing laboratory
- To replace the quartz glass windows with steel plates

Therefore, the glass windows were replaced by removable steel plates, which were manufactured at the mechanical workshop. A request for installation of exhaust fume hoods in testing laboratory was made to the Qatar University Building Operations Department, which took around three months to complete. Meanwhile, the steel enclosure was also arranged from the QU Facilities Department and installed in the laboratory, which also took around 3 weeks to complete. As a result of installation of safety enclosure, all the wiring for the operating controls, switches, lambda sensor and compressor piping had to be done again, to be extended outside the steel enclosure.

All these modifications were done as a requirement from the Qatar University Safety Department, as it was not allowed to run the experiment without addressing the concerned comments. Since the aim of this project is to measure flame speed of fuels using pressure transducer signals, the glass windows were replaced by steel plates which can be replaced by quartz windows whenever the suitable premises is available. It may be noted that the project experimental work got delayed by about four months in order to address all the safety concerns, and finally getting the approval for conducting the experiments.

### 3.4 Final Test Rig Design

There have been many trials and errors in the development of the test rig. Many challenges were faced in terms of right parts selection, insulation material, electrical wiring, heating system and overall safety of the test rig. After making several design modifications, the current overall situation of the test rig can be seen in Figure 34.



*Figure 34 - Final test rig design after modifications*

The following points summarize the major developments in the test rig:

- Control boards installed on both sides of the steel support stand to install the fan switches, spark coil, thermostats, and main power switch.
- The pressure transducer selected for experimentation was PCB Piezotronics (Model 116B03) along with PCB 422E35 in-line charge amplifier. The sensors were installed after calibration.
- For heating the bomb, four 8" surface heating elements were installed on side covers. The test rig was able to reach up to 400°C.
- The ignition coil and spark system was designed using a 12V ignition coil, capacitor and a dimmer switch connect to AC mains.
- A lambda sensor was installed for measuring the actual amount of air and fuel mixture in bomb at the time of ignition. Copper tubing with a gate valve were used for sampling pump connection in the lambda sensor.
- A safety cabinet and exhaust fume hoods were installed around the test rig and all controls wiring was extended wiring to ensure safety.
- Lastly, the areas with leakages in the test rig were sealed by using high temperature silicone, near the gaskets, seals and fittings. This was tested by pressurizing the bomb with air and spraying soap solution on certain areas.

This summarizes the test rig design and development stage. The next section will discuss the actual experimentation steps carried out in the developed test rig.



## **CHAPTER 4. EXPERIMENTAL SETUP AND PROCEDURE**

This chapter of the thesis discusses the experimental procedure used for conducting the flame speed measurements. The section starts by explaining the test rig characterization which includes the initial tests, calibrations and startup checks before conducting the actual experiment. There have been several trials and error before coming up with the final procedure for getting successful ignition and combustion of mixture. The last section of this chapter also briefly highlights the flame visualization capability of the test rig, which serves as a validation for proper mixing, combustion and flame propagation inside the bomb.

### **4.1 Test Rig Characterization**

The test rig characterization step involves finding out and testing different specifications of test rig to account for any errors in the measurements. Since, there were many measuring instruments used in this experiment and all of them have certain degree of accuracy. The individual error in the reading of measuring instruments has been accounted for in the experimental calculations. Also, the test rig has a certain degree of error in holding the air pressure, which is also discussed in the pressure leakage testing. The overall efficiency of the bomb to measure the flame speed accurately is affected by all these parameters. Therefore, the individual steps involved in the characterization are discussed next.

#### 4.1.1 Calibration of Thermocouple

The first step before continuing further is to calibrate the K-Type thermocouple mounted on the bomb for temperature measurement. This task was done by using a precision heating gun with a temperature indicator as shown in Figure 35.



*Figure 35 - Thermocouple Calibration*

The thermocouple reading was also compared with a pre-calibrated thermocouple of the IMR gas analyzer, as well as the temperature indicator on the heating gun. The mounted thermocouple was giving accurate reading up to the tested temperature of 550°C.

#### 4.1.2 Maximum Temperature Testing

The next feature that needs to test in the test rig is the maximum temperature it can reach. As mentioned in the previous chapter, the test rig was tested with various heating system configurations. The final test rig design was the four circular heating coils with K-Type thermocouple and display module. The bomb was heating for 30

minutes and then the heaters were switched off, as shown in Figure 36.

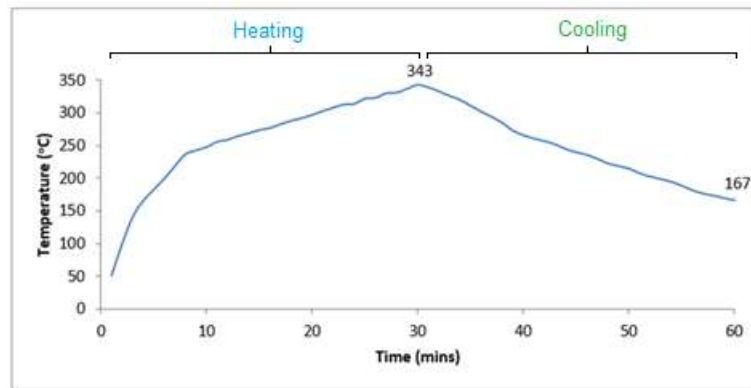
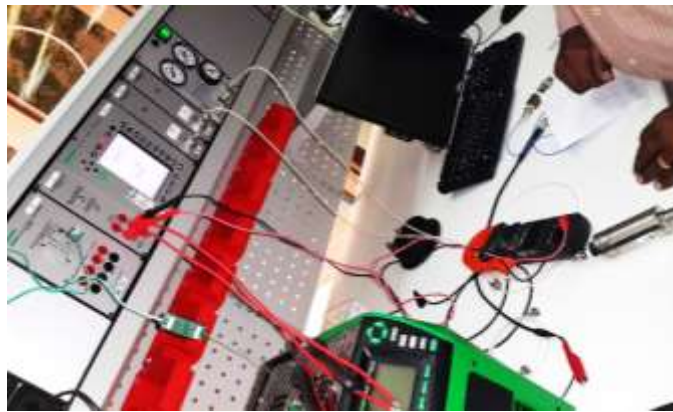


Figure 36 - Temperature vs. time testing

The result shows that the maximum temperature achieved with four heating coils is 343°C in 30 minutes. This is a huge improvement as compared to the previous tests given in chapter 3; i.e. 231°C with two coils. The heating coils were turned off after 30 minutes and the temperature drop was also recorded. The room temperature was 20°C, which shows that the heat loss is gradual. For safe practice, a ceramic insulation pad was placed between the bomb and its support stand to avoid overheating of the electrical wires. It should be noted that the thermocouple has been mounted at the middle of the bomb to be close to the spark location. The bomb easily attains the required temperature range and also goes beyond this temperature if required in the future.

### 4.1.3 Calibration of Pressure Transducer

Even though the calibration charts were provided with the pressure sensor, it was decided to do the re-calibration to test the proper working of the ordered pressure transducer. The calibration was done using a the sensors calibration testing facility available at Qatar University, as shown in Figure 37.



*Figure 37 - Pressure sensor calibration*

The pressure transducer was calibrated by connecting them with the testing machine and a measured amount of pressure was applied. The output signal was recorded and compared with the calibration charts provided with the sensors. Both the pressure sensors were found to be working perfectly and giving correct readings.

### 4.1.4 Setting up the Oscilloscope (DAQ)

After mounting the pressure transducer using adapter fitting and connecting it to the GW-Instek oscilloscope, there was a chance that it will not detect the signal

because of faulty mounting position or any installation damage. Therefore, a purge pressure from the compressor was given to the test rig to check the proper function of the pressure transducer. The pressure transducer reading was found to be in conformity with the pressure given from the compressor with a minor error. Also at this stage, the oscilloscope data logger settings were adjusted to read the signal properly, as shown in Table 4.

*Table 4 - Oscilloscope settings*

<b>Parameters</b>	<b>Settings</b>
Memory Length	25000
Source	CH1
Vertical Units	Volts
Vertical Scale	2.00E-03
Vertical Position	1.60E-03
Horizontal Units	Seconds
Horizontal Scale	1.00E-01
Horizontal Position	0.00E+00
Horizontal Mode	Roll Mode
Sampling Period	4.00E-05

Since there is a sudden rise in pressure in this experiment, the time axis in oscilloscope reader display was set to 100ms. Also the volt axis was set to 100mV in the reader display since the maximum pressure expected in this experiment is 5 bars which comes out to be about 450mV approximately, as shown in Figure 38.

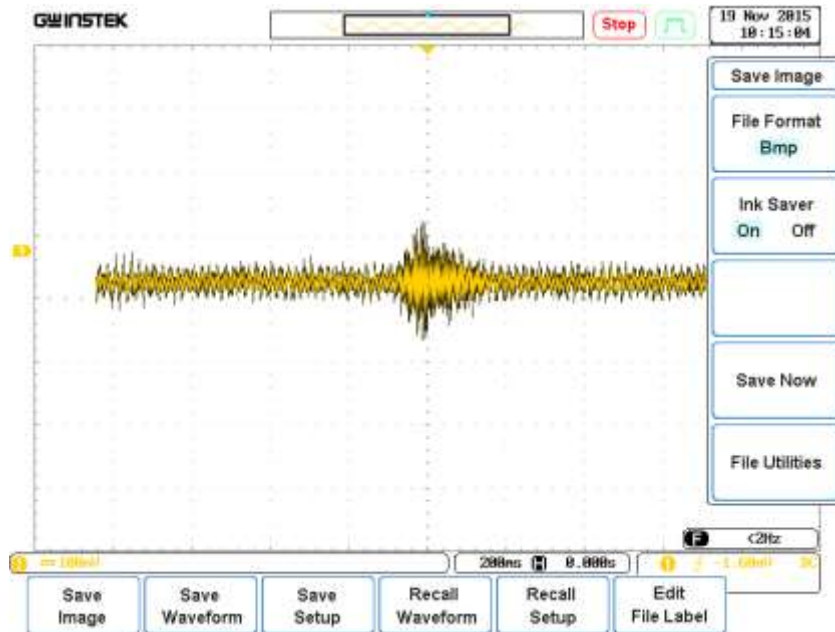


Figure 38 - Oscilloscope reader display settings

As seen in the oscilloscope display, the voltage signal for the given purge pressure is approximately 120mV which converts to around 20psi (1.4bar) gage pressure. The voltage and time data can be extracted from oscilloscope in an MS Excel .CSV file, which make the peak pressure calculation simpler.

Also it can be seen from the reader display that the pressure sensor signal is very sensitive and is displaying noise which has to be smoothed out for getting the peak value of pressure in later analysis. This was done by normalizing the data points in MS Excel, and also by taking the upper envelop values from the data. The detailed calculations for leakage testing are given in the next section.

#### 4.1.5 Pressure Leakage Testing

The next step in testing the test rig before experimentation is confirming if there is any pressure leakage in the bomb. Since this is a constant volume bomb, so the mass of air inside the bomb should remain the same when we heat the test rig from room to higher temperatures. With the increase in temperature, the air will expand and build pressure inside the bomb. This pressure will be checked by pressure transducer and then compared with hand calculations for ideal conditions.

##### Calculations for Moles of Air at Room Temperature:

$$\text{Volume of Bomb} = 0.1374 \text{ m}^3$$

Assuming Ideal Gas Case for Constant Volume of Air

$$\text{Temperature} = T = 293.15 \text{ K}$$

$$\text{Ideal Gas Const.} = R = 8.314 \text{ m}^3\text{Pa}/(\text{mol K})$$

$$\text{Volume} = V = 0.1374 \text{ m}^3$$

$$\text{Pressure} = P = 101345 \text{ Pa (Atmospheric)}$$

$$\text{Moles of Air} = n_{\text{air}} = (PV) / (RT)$$

$$n_{\text{air}} = 5.713 \text{ mol}$$

This is the moles of air at STP conditions inside the bomb. The moles of air calculated at STP and at higher temperatures should be the same because this is a constant

volume case. This can be verified by taking the pressure reading by transducer at STP and at higher temperatures, and then calculating moles of air based on the pressure transducer reading. In this way, the amount of leakage in the bomb can be quantified with this analysis.

For this purpose, all the ports of the bomb were closed and the bomb was heated. Three readings for pressure were taken at three different temperatures using oscilloscope. The pressure transducer output was in millivolts, which was converted to Pascal using the calibration chart provided by the manufacturer.

The scale on the oscilloscope was set as:

- Y-Axis: Volts/Div: 500mV
- X-Axis: Time/Div: 500ms

The first reading was taken at 20°C (or 293.15 K). The corresponding MS Excel .CSV file for oscilloscope reading was used and the voltage signal was converted to pressure signal. The pressure transduced gave a range of readings over time. The most repeating value (mode) of the pressure was taken from these values.

- Pressure at 20°C = 75878 Pa [1<sup>st</sup> Reading]
- Pressure at 180°C = 127795.52 Pa [2<sup>nd</sup> Reading]
- Pressure at 200°C = 131789.13 Pa [3<sup>rd</sup> Reading]



Now these pressure values were used in the Idea Gas Equation to find out the number of moles of air, in an Excel solver, as shown in Figure 39.

Temperature (°C)	Pressure (Pa)	Moles of Air (mol)
20	75878	4.2776248
180	127795.52	4.6606915
200	131789.13	4.6031747

Figure 39 – MS Excel solver for moles of air at 20oC, 180oC and 200oC

The results from this characterization are summarized in Table 5.

Table 5 - Pressure leakage testing results

Parameters	Hand Calculations	Reading 1 At 20°C	Reading 2 At 180°C	Reading 3 At 200°C
Temperature (°C)	20	20	180	200
Pressure (Pa)	101345	75878	127795.52	131789.13
Moles of Air (mol)	5.713	4.277	4.66	4.603

It is obvious from the results that the measured value of moles of air inside the bomb using pressure transducer is slightly less than the hand calculations. There could be two major reasons for this difference:

- The bomb was assumed to be perfectly sealed constant volume chamber. But there is leakage near the fans connection and test rig ports. The leakage could result in not building up the pressure perfectly inside the bomb.
- Error in the calibration of the pressure transducer or slightly higher pressure near the pressure pick up point could also result in faulty reading.

In any case, one that can be deduced from this experiment is that the number of moles of air inside the bomb is almost constant as the temperature is increased from 20°C to 200°C. The slight variation in this value gives an indication of the amount of leakage inside the test rig. Moreover, the actual air to fuel ratio at the moment of ignition during the experiment has been measured by the lambda sensor.

## **4.2 Final Experimental Procedure**

The proposed experimental procedure was not giving proper ignition of the mixture. After conducting the experimental runs with conventional diesel according to the proposed procedure, the steps were slightly modified and tried again. The following experimental procedure gave the successful ignition for each experimental run:

- The bomb was flushed with air using a compressor with exhaust port open
- All the ports were closed and the heaters were switched on
- The temperature of the bomb was allowed to reach 250°C and held at this temperature for 15 minutes
- The bomb was allowed to reach down to the desired initial temperature of 190°C for the first experimental run with diesel
- 6.5 mL of conventional diesel was sprayed into the bomb using a sprayer through a ball-valve to aim for equivalence ratio of 1.0
- The electric fans were switched on for approximately 30 seconds.

- The fans were switched off and the mixture was left for one and half minute to reach a steady equilibrium state and to fully evaporate the fuel
- At this time, the lambda sensor valve was opened and the oxygen percentage was noted down for calculating the actual amount of fuel evaporated and air left inside the bomb
- Before igniting the mixture, the protective cage was closed and it was made sure that no fuel bottles or flammable material is kept near the test rig
- Lastly, the mixture was ignited using the spark ignition coil circuit which was operated from a distance
- The pressure rise signal after igniting the mixture was detected by the pressure transducer connected to the oscilloscope
- The rise in temperature was recorded by the help of thermocouple reader
- The exhaust port of the bomb was opened and burnt gases were removed by flushing the bomb again using air compressor
- After flushing, the test rig is ready for the next test run

The same procedure was repeated many times for each conditions to ensure the repeatability of the results. Also, it was observed in some test runs that the ignition is not occurring after operating the spark coil circuit, especially when aiming at getting equivalence ratios away from the stoichiometric conditions.

### 4.3 Fuels Used

The fuels used in the present study are; conventional diesel, GTL and GTL blends. The data sheet for the GTL fuel, supplied by a local company, is given in Appendix D, while the basic properties of the tested fuels tested are shown in Table 6.

*Table 6 - Properties of fuels used*

<b>Properties</b>	<b>Diesel</b> [34]	<b>GTL</b> [3], [35]	<b>50/50</b> <b>Blend</b>
H/C Ratio	2.125	2.1-2.15	2.1-2.125
Approx. Formula	C <sub>16</sub> H <sub>34</sub>	C <sub>16</sub> H <sub>34</sub>	C <sub>16</sub> H <sub>34</sub>
Density at 15°C (kg/m <sup>3</sup> )	830	770	792
Boiling Range (°C)	190-360	160 - 360	165 - 360
Flash Point (°C)	55	77	71
Centane No.	55	75	64
Calorific Value (MJ/kg)	42.9	49.3	46.2

For the blended fuel, the GTL was mixed with conventional diesel with 50/50 (by volume) proportions. The properties of the blended fuel were determined by the laboratory analysis. The details and results for the diesel, GTL and blended fuel is will be discussed in the next chapter of this thesis.

### 4.4 Flame Visualization Experiment

Although the present work relies on the pressure signal for flame speed measurement, the developed test rig is also suitable for high speed flame imaging. A test run was conducted to verify this by replacing the steel window covers by Quartz

glass. Due to unavailability of the high speed imaging system, a normal video camera was used with to capture the flame. Figure 40 shows a sequence of photos taken at 60 frames per second, for GTL ignited at an initial temperature of 175°C.

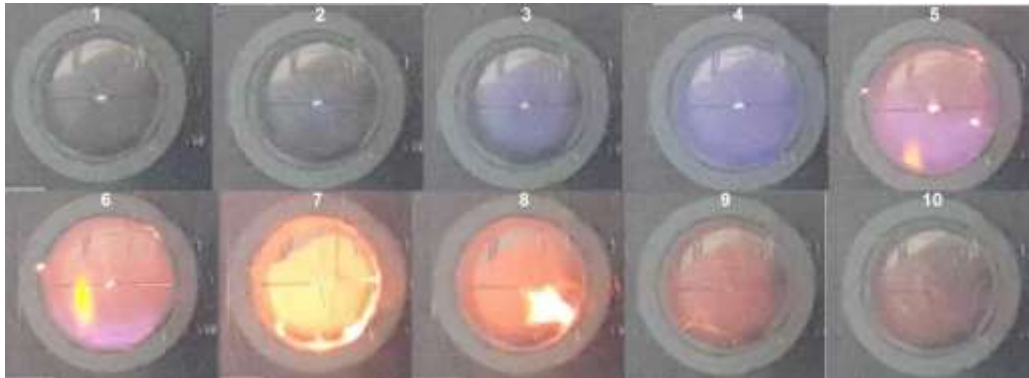


*Figure 40 - Flame visualization*

The first four images shows a blue colored flame spreading evenly towards the surface of the chamber. If this increase in flame radius is analyzed numerically, the flame speed can be obtained. Also it can be observed from the images that when the flame reaches the cylinder walls, the residual fuel droplets get burnt, which appears in image sequence number 7 and 8.

This flame imaging experiment verifies that the desired conditions for proper mixing and spreading of flame have been met inside the bomb. This also verifies that the flame is spreading evenly from the center of the bomb towards the walls.

## **CHAPTER 5. RESULTS AND DISCUSSION**

This chapter of the thesis discusses the results obtained as a result of experimental runs of the combustion bomb test rig. The section starts by explaining the necessary calculations required to analyze the data from the pressure sensor and lambda sensor. Sample calculations were also explained which showed the steps for calculating the equivalence ratio and flame speed from the given raw data and initial conditions. Three categories of results were obtained; i.e. test runs using conventional diesel, GTL, and a 50/50 blend for conventional diesel and GTL, as well as, measuring the flame speeds at different initial temperatures. The first set of results for conventional diesel were important to validate the accuracy of the test rig and experimental procedure by comparing them with the previous work done on diesel fuel. The second set of results are important to fill the knowledge gap in the research work regarding the GTL fuel.

### **5.1 Conventional Diesel**

The first set of experimental runs were conducted using the conventional diesel as test fuel. The initial temperature of the test rig was kept at 190°C. The amount of fuel injected in the test rig was approximately 6.5L, to aim at getting an equivalence ratio close to 1.0.

### 5.1.1 Pressure Sensor Data Interpretation for Diesel Tests

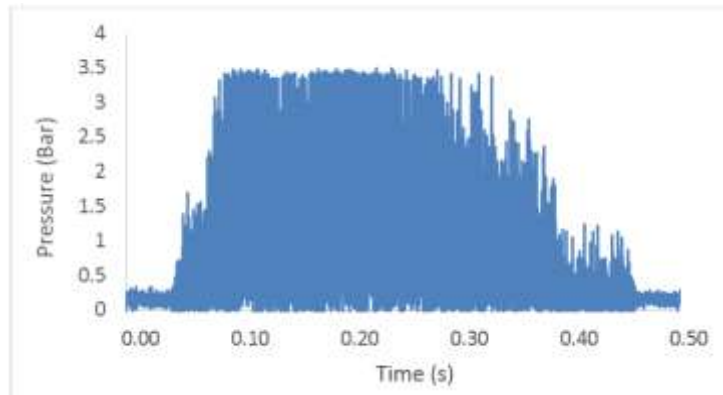
The data for the first experimental run using diesel fuel is summarized in Table 7.

Table 7 - Test details

Test Details	
Fuel Type	Diesel
Initial Temp (°C)	190
Initial Pressure (Bar)	1.1
O <sub>2</sub> Sensor Reading (% age):	20.1
Peak Voltage (mV)	303
Peak Relative Pressure (psi)	48.57
Pressure Calibration (mV/psi)	6.239
Peak Relative Pressure (bar)	3.35

The test details were necessary to record in order to proceed with further calculations. The voltage (mV) signal captured by the oscilloscope is saved in the .CSV format. The pressure is calculated by converting the signal (mV) from the oscilloscope into pressure using the calibration data of the pressure sensor. This calculation is fairly simple as explained in chapter 4, and the pressure is obtained by multiplying the calibration factor (mV/psi) by the voltage signal (mV).

Using this calibration factor, the .CSV data file obtained from pressure sensor for the full range of signal is converted into pressure using MS Excel and plotted in the form of a graph as shown in Figure 41.



*Figure 41 - Raw signal of pressure*

Note that the original voltage signal had noise, which was smoothed out by normalizing the data and then performing an upper envelope extraction to get the peak signals. So, the final form of pressure and time curve is shown in Figure 42.

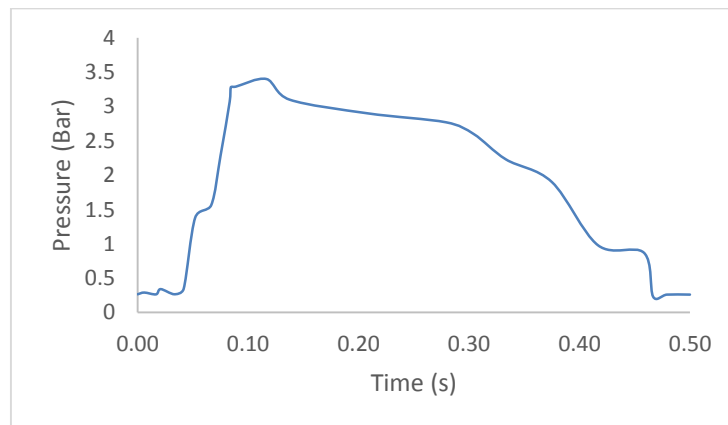


*Figure 42 - Pressure vs. time plot for diesel at 180 °C*

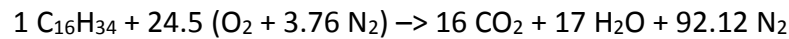
This plot of pressure and time is used to obtain the peak pressure, which came out to be 3.35 Bar. The flame speed can be calculated from this data but it is essential to determine the equivalence ratio at which the ignition took place, as explained next.



### 5.1.2 Equivalence Ratio Calculations for Diesel Tests

The equivalence ratio shows the condition of the air and fuel mixture, whether it is lean, stoichiometric or rich. The equivalence ratio at which, the experiment is taking place needs to be calculated for studying the effect of change in equivalence ratio on the flame speed. The following steps show the procedure for calculating the equivalence ratio from the lambda sensor reading, for the diesel fuel injected in this test run.

The balanced chemical reaction for 1 mol of any Diesel is given by:



$$\begin{aligned} \text{Mass of Fuel:} \quad m_{\text{fuel}} &= n_{\text{fuel}} \times M.M_{\text{fuel}} = 1 \times M.M_{\text{fuel}} \\ m_{\text{fuel}} &= 226 \text{ g} \end{aligned}$$

$$\begin{aligned} \text{Mass of Air:} \quad m_{\text{air}} &= [n_{\text{O}_2} \times M.M_{\text{O}_2}] + [n_{\text{N}_2} \times M.M_{\text{N}_2}] \\ m_{\text{air}} &= [n_{\text{O}_2} \times M.M_{\text{O}_2}] + [n_{\text{O}_2} \times (79/21) \times M.M_{\text{N}_2}] \\ m_{\text{air}} &= 3364.67 \text{ g} \end{aligned}$$

$$\begin{aligned} \text{Air-Fuel Ratio (Stoic): } (A/F)_{\text{stoic}} &= m_{\text{air}} / m_{\text{fuel}} = 3364.67 / 226 \\ (A/F)_{\text{stoic}} &= 14.89 \end{aligned}$$

$$\text{Equivalence Ratio: } \Phi = (A/F)_{\text{stoic}} / (A/F)_{\text{actual}}$$

For  $(A/F)_{\text{actual}}$ , the actual amount of air and fuel injected in bomb will be considered.

The reading from lambda sensor is used to estimate the actual amount of air present in bomb and the amount of fuel evaporated which is available for combustion.

**Mass of Air in Bomb (Before injecting fuel):**

$$\text{Bomb Vol} = V_{\text{bomb}} = 0.1374 \text{ m}^3$$

$$\text{Air Density @180 }^\circ\text{C} = \rho_{\text{air}} = 0.75 \text{ kg/m}^3$$

$$\text{Mass of air in bomb} = m_{\text{air}} = 102.50 \text{ g}$$

$$\text{Molar Mass of air} = M_{\text{air}} = 28.96 \text{ g/mol}$$

$$\text{Moles of air in bomb} = n_{\text{air}} = 3.54 \text{ mol}$$

**Mass of Fuel Injected in Bomb:**

$$\text{Vol-fuel injected} = V_{\text{fuel}} = 6.5 \text{ mL} = 0.0000065 \text{ m}^3$$

$$\text{Density Fuel} = \rho_{\text{fuel}} = 770000 \text{ g/m}^3$$

$$\text{Mass of Fuel} = m_{\text{fuel}} = V_{\text{fuel}} \times \rho_{\text{fuel}}$$

$$m_{\text{fuel}} = 5.005 \text{ g}$$

Now, the lambda sensor is reading a slightly lower percentage of oxygen after injecting fuel, i.e. 19.8% O<sub>2</sub>. This means that total volume of air in bomb is shared with some volume of fuel evaporated inside the bomb after injection. Therefore, the actual mass of air and fuel has to be calculated based on lambda sensor reading.

**Actual Mass of Air and Fuel (Corrected by Lambda Sensor):**

Assuming that 19.8% O<sub>2</sub> means that 100 moles of Air has 19.8 moles of O<sub>2</sub>. Now, the following calculation is done to get actual mass of air (m-air) for the moles of air in

bomb based on lambda sensor reading.

$$\text{O}_2 \text{ Sensor Reading} = \text{O}_2\% = 19.8 \%$$

$$\text{Moles of Air in bomb} = n_{\text{air}} = 3.54 \text{ mol}$$

$$\text{Moles of O}_2 \text{ Actual} = n_{\text{O}_2} = n_{\text{air}} \times \text{O}_2\% = 0.701 \text{ mol}$$

$$\text{Mass of Air Actual} = m_{\text{air actual}} = n_{\text{O}_2} \times (M.M_{\text{O}_2} + (79/21) \times M.M_{\text{N}_2})$$

$$m_{\text{air actual}} = 0.701 \times (32 + (79/21) \times 28)$$

$$m_{\text{air actual}} = 96.260 \text{ g}$$

$$\text{Density of air} = \rho_{\text{air}} = 0.75 \text{ kg/m}^3$$

$$\text{Vol-Air Actual (after fuel injection)} = m_{\text{air actual}} \times \rho_{\text{air}} = 0.129 \text{ m}^3$$

$$\text{Vol-fuel Actual (shared with Air)} = V_{\text{bomb}} - V_{\text{air actual}}$$

$$V_{\text{fuel actual}} = 0.008 \text{ m}^3$$

$$m_{\text{fuel actual}} = 6.44 \text{ g}$$

$$\text{Air-Fuel Ratio Actual: } (A/F)_{\text{actual}} = 14.94 \text{ g}$$

$$\text{Equivalence Ratio: } \Phi = (A/F)_{\text{stoic}} / (A/F)_{\text{actual}} = 14.89 / 14.94$$

$$\Phi = 1.0$$

This is the equivalence ratio at which the combustion occurs, which is 1.0. This shows that the mixture is at stoichiometric conditions. If this value of less than 1, the mixture is lean; and if this value is greater than 1, the mixture is rich.

### 5.1.3 Summary of Results for Equivalence Ratios from Diesel Fuel Tests

Using the above calculations methodology, an MS Excel calculator is developed which can be used to find out the equivalence ratios for different initial conditions in each experimental trial. The summary of these calculations is shown in Table 8.

Table 8 - Equivalence ratio calculations summary - diesel

O <sub>2</sub> %	Actual Mole of O <sub>2</sub> (mol)	Actual Mass of Air (g)	V-Fuel Injected (mL)	m-fuel injected (g)	m-fuel evap (g)	(A/F) Actual	$\Phi$
20.4	0.72	99.18	5	3.85	3.43	28.91	0.5
20.3	0.72	98.69	5.3	4.08	3.93	25.1	0.6
20.2	0.72	98.2	6	4.62	4.43	22.15	0.7
20.1	0.71	97.72	6.5	5.01	4.94	19.8	0.8
19.9	0.7	96.75	8	6.16	5.94	16.29	0.9
19.8	0.7	96.26	9	6.93	6.44	14.94	1
19.7	0.7	95.77	9.3	7.16	6.94	13.79	1.1
19.6	0.69	95.29	10	7.7	7.45	12.8	1.2

Note that a specific volume of fuel has to be injected in the test rig for targeting the required equivalence ratio. There were a lot of trials and errors before finding out the amount of fuel required for the desired actual amount of evaporated fuel available for combustion. As seen in the table, amount of fuel evaporated is slightly less than the amount injected. This could be due to the fact that a few fuel droplets have condensed and trapped in fuel injection lines or near the crevices of the bomb.

The MS Excel equivalence ratio calculator sheet is provided in Appendix A.

#### 5.1.4 Flame Speed Calculations for Diesel Tests

The pressure data obtained from the pressure sensor is used for flame speed calculation. There are several equations used to this purpose, as mentioned in the literature review. In this thesis, the laminar flame speed is calculated from the pressure versus time record as proposed by Lewis and Von Elbe [36]. The same model has been used earlier in a similar research [35], where the flame speed of diesel fuel is compared with Jojoba methyl ester using cylindrical bomb method relying on pressure transducer reading for flame speed calculations. The set of equations relating the burning velocity to the instantaneous values of the pressure are given in Table 9.

Table 9 - Equations for flame speed calculation [35]

Main Equation	$S_N = (dr_i/dt) (r_i/r_b)^2 (P_i/P)^{(1/\gamma_u)}$
Sub Eq (i)	$dr_i/dt = (R/3(P_e-P_i))[(P-P_i)/(P_e-P_i)]^{(2/3)} (d_p/dt)$
Sub Eq (ii)	$r_i = R [(P-P_i)/(P_e-P_i)]^{(1/3)}$
Sub Eq (iii)	$r_b = R [1-(P_i/P)(T_u/T_i)(P_e-P)/(P_e-P_i)]$
Sub Eq (iv)	$(T_u/T_i) = (P/P_i)^{(1/\gamma_u)}$

The values for the parameters mentioned in the equations were taken by direct measurements from the instruments installed on the test rig. The individual parameters are given in the nomenclature section of the thesis. The MS Excel calculator, given in Table 10, shows a sample calculation of the flame speed.

Table 10 - Flame speed calculations

Test Fuel: Diesel at 190°C		
Parameter	Symbol (Units)	$\Phi = 1.0$
Radius of Bomb	R (m)	0.4
Pressure - Initial before combustion	$P_i$ (Pa)	110000
Pressure - Equilibrium Burned Gases	$P_e$ (Pa)	113000
Pressure - Peak during combustion	P (Pa)	358000
Temperature - Burnt Gas	$T_u$ (K)	484.15
Temperature - Initial Mixture	$T_i$ (K)	454.14
Slope - Pressure vs. Time Curve	$(dp/dt)$	36.9
1st Equation	$dr_i/dt$	0.76
2nd Equation	$r_i$	1.74
3rd Equation	$r_b$	11.1
4th Equation	$(p/pi)^{(1/\gamma_u)}$	1.07
<b>Laminar Flame Speed</b>	<b><math>S_N</math> (cm/s)</b>	<b>73.58</b>

As seen in Table 10, the initial conditions (parameters) as well as final conditions of the test are specific for each test run. Therefore, the calculations for each test run had to be done separately. A summary of the results is given in next section and the MS Excel flame speed calculator sheet is attached in Appendix B.

### 5.3.1 Summary of Results for Flame Speed for Diesel Tests

The summary of flame speed was calculated for a range of equivalence ratios (from 0.7 to 1.3) for diesel fuel is given in Table 11.

Table 11 - Diesel test results summary

Test #	Test Conditions	$\Phi$	Max P (Bar)	$S_N$ (cm/s)
1	Pure Diesel, $T_i=190$ oC	0.7	2.29	49.2
2	Pure Diesel, $T_i=190$ oC	0.8	2.9	59.82
3	Pure Diesel, $T_i=190$ oC	0.9	3.27	67
4	Pure Diesel, $T_i=190$ oC	1	3.8	78.33
5	Pure Diesel, $T_i=190$ oC	1.1	4.02	83.19
6	Pure Diesel, $T_i=190$ oC	1.2	3.95	81.63
7	Pure Diesel, $T_i=190$ oC	1.3	3.9	80.34

These results were used to plot the equivalence ratio against the flame speed as shown in Figure 43.

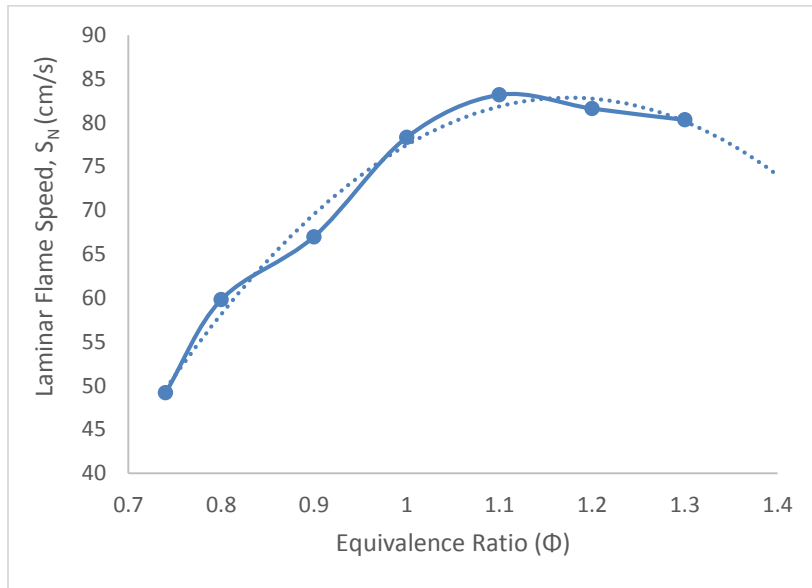


Figure 43 - Results for pure diesel ( $S_N$  vs.  $\Phi$ )

It was observed in the diesel tests that the flame speed is relatively low at lean mixture ( $\Phi=0.7-0.9$ ), increases and peaks near stoichiometric conditions ( $\Phi=1.0-1.1$ ), and decreases at rich mixture ( $\Phi=1.2-1.3$ ). Note that there were multiple

experimental runs for the same equivalence ratio before getting the results. This is because it was not possible to get ignition each time, especially when aiming for the equivalence ratios away from the stoichiometric conditions. This is explained more in the repeatability test section next. The trends for variation of flame speed with the equivalence ratio for the diesel tests will be used for validation of the experimental results in the next section.

## **5.2 Validation of Results using Diesel Tests**

The results obtained from the diesel test runs have to be validated, as this is a newly developed test rig. The flame speed of diesel fuel, in the present work, was measured at various equivalence ratios to compare it with the already established data in open literature. Also a series of tests were performed to check the repeatability of the experimental results

### **5.2.1 Comparison with Existing Work**

For validation purpose, the research work of Chong and Hochgreb [37] was taken because this recent work also uses the diesel fuel with similar properties and testing environments. But the initial temperature for these tests is 196°C. Therefore, the correlation for flame speed variation with temperature, suggested by Radwan *et.al* [35], was used to obtain the values mentioned in literature exactly at 190°C, which is the same as the present test conditions. The values from, the previous research and



present work, for the flame speed were plotted against a range of equivalence ratios, as shown in Figure 44.

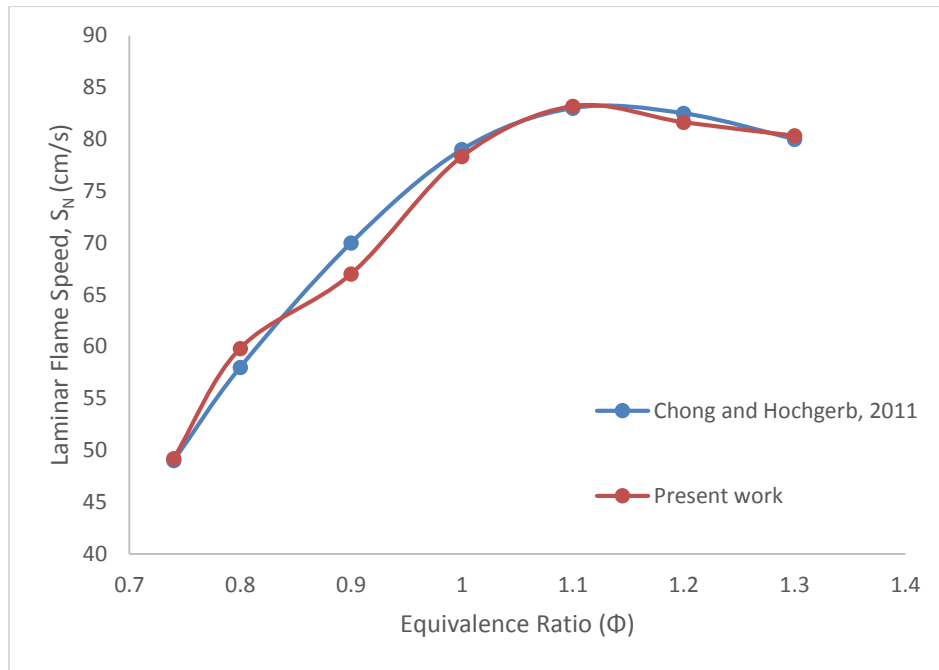


Figure 44 - Test rig results validation

It can be seen that the flame speed values in the present work are following the same trend as the existing work. The  $S_N$  values at all the points are within 1% to 1.5% error, except for the  $S_N$  value at  $\Phi=0.9$ , where there is a difference of 3 cm/s (4% error) between the existing and present work. This could be because of the difference in the testing environments. The present work employs a newly designed test rig, which can be different in the many forms like; volume of bomb, number of crevices, uniform temperature throughout the bomb, and complete evaporation of fuel. All these factors can lead to the observed difference in results.

### 5.2.2 Repeatability Test

In order to confirm the repeatability of results, the test rig was operated at the same initial conditions for three days, with two readings per day. Again, the diesel fuel was selected for this purpose, which was ignited at  $\Phi=1.1$ , an initial temperature of  $190^{\circ}\text{C}$ , and at atmospheric pressure. The corresponding flame speeds for these tests were recorded, as given in

Table 12 - Repeatability test results

Property Measured	Day 1		Day 2		Day 3		Mean	St. Dev	Standard Error %
	Test 1	Test 2	Test 1	Test 2	Test 1	Test 2			
$\Phi$	1.09	1.11	1.12	1.10	1.09	1.10	1.10	0.012	1.1%
$S_N$ (cm/s)	83.19	83.47	83.52	82.78	82.93	83.45	83.22	0.311	0.4%

It can be noted that the standard error for the six equivalence ratio ( $\Phi$ ) readings over three days is 1.1%, while the standard error for the flame speed ( $S_N$ ) measurement is 0.4%. The values indicate a decent repeatability precision for the experimental setup.

## **5.3 Pure GTL**

As mentioned in the final experimental procedure, the GTL test runs were conducted in the same way as the conventional diesel tests. The equivalence ratio calculations were similar in most respects as the H/C ratio for GTL and Diesel fuel were approximately the same [5], as shown in Table 6 earlier. The flame speed calculations were also the same, as they rely on the pressure signal. The results were slightly different as the chemical properties of GTL are different from that of the conventional diesel.

It is important to highlight here that the mixtures for GTL experimental runs were much easier to ignite and there was a lot less trials, as compared to the conventional diesel. This could be due to the fact that the GTL starts boiling from 160°C while conventional diesel starts boiling after 190°C. This could have accounted for less effect of wall cooling at the time of fuel injection. Also, it was noted that the exhaust gases after evacuating the bomb were colorless. This could be because of close to zero Sulphur content in the clean GTL.

### **5.3.1 Summary of Results for GTL Tests**

The results for equivalence were obtained from the lambda sensor reading, from an equivalence ratio of 0.7 to 1.3. After that, the corresponding flame speed was calculated for experimental trial. A summary of the results of the GTL fuel test runs

is given in Table 13.

Table 13 - GTL test results summary

Test #	Test Conditions	$\Phi$	Max P (Bar)	$S_N$ (cm/s)
1	GTL, Ti=190 °C	0.7	2.76	55.1
2	GTL, Ti=190 °C	0.8	2.9	57.04
3	GTL, Ti=190 °C	0.9	3.7	71.15
4	GTL, Ti=190 °C	1	4.3	84.26
5	GTL, Ti=190 °C	1.1	4.5	88.3
6	GTL, Ti=190 °C	1.2	4.2	86
7	GTL, Ti=190 °C	1.3	3.98	79

### 5.3.2 Effect of Varying the Equivalence Ratio of GTL

As shown in Table 13, the data for equivalence ratio and flame speed for GTL shows that there is a variation in the flame speed when the equivalence ratio is changed.

Therefore, Figure 45 is plotted to visualize the trends clearly.

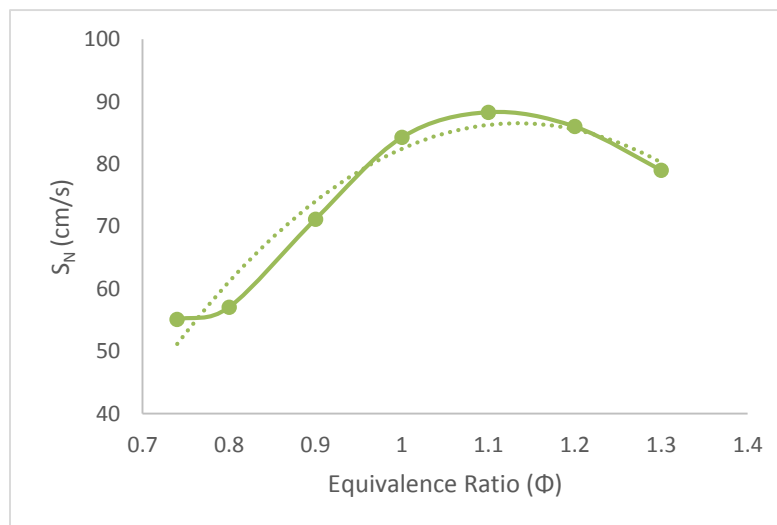


Figure 45 - Results of GTL ( $S_N$  vs.  $\Phi$ )

It can be seen that the flame speed is very low, about 55 cm/s, in lean mixture conditions. At stoichiometric conditions, the flame speed peaks to 88.3 cm/s having an equivalence ratio of 1.1. Again, in fuel rich conditions, the flame speed gradually drops. The trend for rise and drop of the flame speed is found similar to the conventional diesel fuel. The actual comparison and discussion for the results of all tested fuels is given at the end of this chapter.

### 5.3.3 Effect of Varying the Initial Temperature of GTL

Another sort of investigation was carried out with the GTL fuel, which is varying the initial temperature of the mixture. In the literature, it was found that changing the initial temperature of the mixture also affects the flame speed of the mixture.

The equivalence ratio for this study was kept at 1.0. The fuel was ignited at three different temperatures, i.e. 190°C, 220°C and 250°C. The corresponding laminar flame speed was measured by getting the pressure signal. Table 14 summarizes the results obtained from this investigation.

*Table 14 – GTL initial temperature variation*

Test #	Test Conditions	T <sub>i</sub> (°C)	S <sub>N</sub> (cm/s)
1	GTL, $\Phi = 1.0$	190	84.3
2	GTL, $\Phi = 1.0$	220	87.4
3	GTL, $\Phi = 1.0$	250	94.2

It can be seen from the results that the flame speed is increasing with the increase in

temperature. Also it is important to highlight the tests conducted at 220°C and 250°C were successful in the first trial, as the mixture was at higher temperature.

A similar test was also done for the 50/50 (by volume) blend of GTL and conventional diesel, which will be compared with this result at the end of this chapter.

#### **5.4 GTL and Conventional Diesel Blend**

After investigating the GTL, the investigation was further enriched by studying the trends for blended fuel. This is because most of the industry is using GTL blended with the conventional fuels. The idea is to have the positive characteristics of new fuel along with the economy of using the conventional fuel combined together to give optimum fuel blend.

Therefore, the blended fuel investigated was GTL mixed with conventional diesel in 50%/50% proportions by volume. After preparing and analyzing the blended fuel, the experimental test runs were conducted in the same way as the conventional diesel and GTL tests.

It is important to highlight here that the blended fuel mixtures in some trials were harder to ignite at 190°C, similar to what was experienced in the experimental runs with conventional diesel. But in some trials, the blended fuel ignited in the first attempt. This could be due to the fuel separation in the blend. This may result in

irregular ignition behavior. The exhaust smoke observed was not as black as the conventional diesel but there was a light grey color in the smoke.

#### 5.4.1 Summary of Results for 50/50 Blend Tests

The results for equivalence were obtained from the lambda sensor reading, from an equivalence ratio of 0.7 to 1.3. After that, the corresponding flame speed was calculated for experimental trial. A summary of the results of the blended fuel test runs is given in Table 15.

*Table 15 – 50-50 blend results summary*

Test #	Test Conditions	$\Phi$	Max P (Bar)	$S_N$ (cm/s)
1	50-50 Blend, $T_i=190\text{ }^\circ\text{C}$	0.7	2.42	50.9
2	50-50 Blend, $T_i=190\text{ }^\circ\text{C}$	0.8	2.66	54.02
3	50-50 Blend, $T_i=190\text{ }^\circ\text{C}$	0.9	3.25	65.35
4	50-50 Blend, $T_i=190\text{ }^\circ\text{C}$	1	3.9	80.09
5	50-50 Blend, $T_i=190\text{ }^\circ\text{C}$	1.1	4.15	85.4
6	50-50 Blend, $T_i=190\text{ }^\circ\text{C}$	1.2	4.0	83.1
7	50-50 Blend, $T_i=190\text{ }^\circ\text{C}$	1.3	3.8	77.8

#### 5.4.2 Effect of Varying the Equivalence Ratio 50/50 Blend

As shown in Table 15, the data for equivalence ratio and flame speed for blended fuel shows that there is a variation in the flame speed when the equivalence ratio is changed, which can be seen in Figure 46.

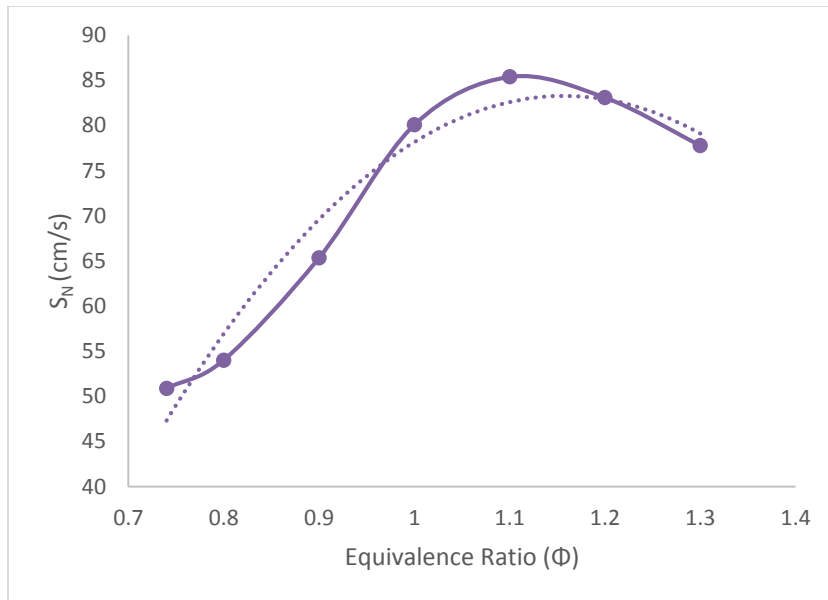


Figure 46 - Results of 50-50 blend ( $S_N$  vs.  $\Phi$ )

Like the previous two fuels, the flame speed is very low, about 50.9 cm/s, in lean mixture conditions. At stoichiometric conditions, the flame speed peaks to 85.4 cm/s having an equivalence ratio of 1.1. Again, in fuel rich conditions, the flame speed gradually drops. The actual comparison and discussion for the results of all tested fuels is given at the end of this chapter.

#### 5.4.3 Effect of Varying the Initial Temperature of 50/50 Blend

The test runs with different initial temperatures were also conducted for 50/50 blend, and the resulting flame speeds were recorded. The test conditions were kept similar to the GTL tests in order to make a good comparison between the fuels. The results for this investigation are summarized in Table 16.



Table 16 – 50-50 blend initial temperature variation

Test #	Test Conditions	T <sub>i</sub> (°C)	S <sub>N</sub> (cm/s)
1	50-50 Blend, $\Phi = 1.0$	190	80.1
2	50-50 Blend, $\Phi = 1.0$	220	85.3
3	50-50 Blend, $\Phi = 1.0$	250	89.7

It can be seen from the results that the flame speed is increase with the increase in temperature. But it is noted that the increase in flame speed is not as much as the GTL. The trends will be compared and discussed in the next section.

## 5.5 Comparison of Results for the Tested Fuels

After carrying out individual tests and analyzing the recorded values, a comparison between the three tested fuels; i.e. conventional diesel, GTL, and 50/50 blend, is necessary in order to establish some relationships and to see the trends.

### 5.5.1 Effect of Equivalence Ratio Variation on the Flame Speed

The first comparison made was comparing the plots for equivalence versus flame speed for the three fuels. This is very important study as this can give an idea which fuel is performing better and giving the highest flame speed and at certain mixture conditions. Therefore, a plot for investigating the effect of changing the equivalence ratio on the flame speed, for the three tested fuels is shown in Figure 47.

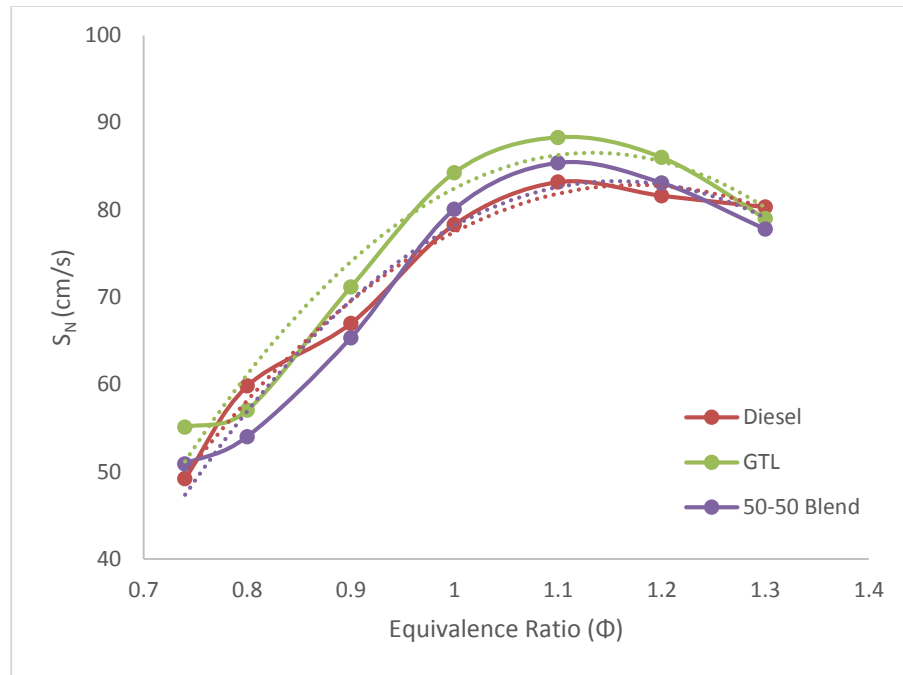


Figure 47 - Conventional Diesel, GTL and 50-50 Blend ( $S_N$  vs.  $\Phi$ )

As seen in the plot, the GTL has the highest flame speed as compared to conventional diesel and 50/50 blend, near and at stoichiometric conditions ( $\Phi = 1$ ). As the equivalence ratio of mixture gets away from the stoichiometric conditions, the flame speed of the GTL gets slightly lower than the conventional diesel. The higher flame speed of the GTL could be the result of its higher calorific value as compared to both fuels. From this, it can be concluded that the GTL can be a potential alternative fuel for applications where the running conditions are near stoichiometric and as such, using GTL fuel can give result in higher flame speeds. But this is of course, after further investigating the chemical kinetics as well as other physical factors into account.

The behaviors of 50/50 blend is quite interesting when compared to both pure fuels. At lower equivalence ratio, it starts with the lowest flame speed and stays low until it approximately equalizes with the conventional diesel at equivalence ratio of 1.0. At 1.1, the flame speed is only 2-3 cm/s higher than the conventional diesel. After that, the flame speed again drops lower than both fuels. It can be seen that the 50/50 blend is exhibiting lower flame speed than both fuels away from stoichiometric conditions. Near stoichiometric conditions, 50/50 blend is performing almost similar to conventional diesel, which is a green signal for industries to use the cleaner GTL blended with conventional diesel to improve their emissions.

For the three tested fuels, excess air is causing flame quenching when the mixture is lean which is resulting in lower laminar flame speeds, and excess fuel is causing incomplete combustion when the mixture is rich resulting in lower flame speeds.

### **5.5.2 Effect of Initial Temperature Variation on the Flame Speed**

The second comparison between the three tested fuels is investigating the effect of initial temperature variation on the flame speed. For this, the tests were conducted at higher initial temperature of mixture before combustion. A summary of the results of these test is shown in Table 17.

Table 17 - Effect of initial temperature variation

Test #	$\Phi$	$T_i$ (°C)	Pure Diesel $S_N$ (cm/s)	GTL $S_N$ (cm/s)	50-50 Blend $S_N$ (cm/s)
1	1	190	78.3	84.3	80.1
2	1	220	84.7	87.4	85.3
3	1	250	90.1	94.2	89.7

Also, plot showing the effect of increase in initial temperature is constructed to visualize and compare the trends of pure diesel, GTL and blended fuel, as shown in Figure 48.

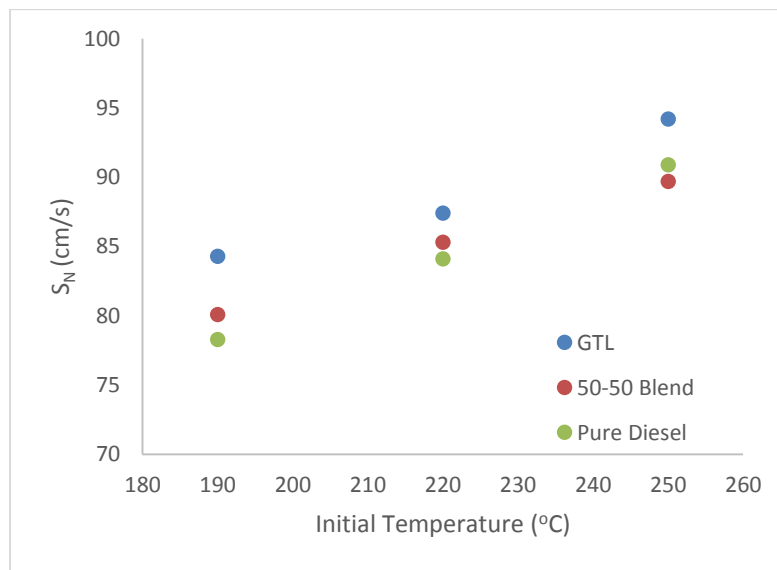


Figure 48 - Effect of changing initial temperature for GTL and 50-50 blend

It can be observed in the plot that the flame speed is increasing almost linearly with the increase in initial temperature of the mixture for all the three tested fuels. This linearity behavior has been observed before in similar investigations [35]. This is

because at increased temperatures, the rate of reaction is increased resulting in higher flame speeds. The following observations can be made from the above results.

- The flame speed is increasing with the increase in temperature in a linear behavior.
- Pure diesel and GTL are exhibiting a similar pattern and the increase in flame speed at 250°C, is slightly higher than the increase at previous points.
- The trend for the 50/50 blend is linear as compared to the trends of other two fuels. This might be because of non-uniform mixture or fuel separation as this is a blended fuel. In addition, this could be a result of incomplete combustion for this specific test value.
- The tests need to be conducted at even higher temperatures but due to the time limitations, this could not be done.

The above results show that blended GTL with conventional diesel does not affect much the laminar flame speed of the diesel fuel at different equivalence ratios and initial temperature. However, the laminar flame speed of GTL as a pure fuel is higher than those of diesel fuel and 50/50 blends, especially at stoichiometric and slightly rich mixtures. This is an interesting finding from this study. The reason behind this behavior has to be investigated with chemical kinetics in order to understand how the chemical reaction behaves when the 50/50 blended fuel ignites.

## **CHAPTER 6. CONCLUSIONS AND RECOMMENDATIONS**

### **6.1 Conclusions**

In conclusion, this thesis investigates the flame speed of GTL fuel along with its blends with conventional diesel, in a newly designed and manufactured cylindrical bomb test rig. A detailed justification was presented that being the largest producer of GTL products, Qatar should be in the leading position for pioneering the research in GTL blended fuel characteristics. Previous research works employing spherical bomb technique were reviewed in detail and the new test rig design was developed based on their recommendations.

The proposed test rig for the measurement of GTL fuel blends flame speed is a state of the art design and can be used to measure laminar as well as turbulent flame speeds. Also, it can employ pressure signal as well as high speed imaging for better accuracy in measurement of the flame speeds. A detailed description of steps for the design and development of test rig were given. All the measuring instruments and calculations involved for getting the final results were also explained.

Firstly, the conventional diesel fuel was tested for flame speeds at different equivalence ratios and it was found within the 1.5% of the values mentioned in the literature. Based on the same methodology, the flame speed of GTL and 50/50 blend of conventional diesel and GTL was measured in the same test rig, and the following

results were obtained for the effect of change in equivalence ratio on flame speed.

- GTL has highest flame speed near stoichiometric conditions, i.e. 88.3 cm/s at  $\Phi=1.1$ , which is 5 cm/s more than conventional diesel
- At lean and rich mixtures, the flame speed of GTL is lower than conventional diesel, by 2-4 cm/s
- The 50/50 blend gave a lower flame speed at lean and rich mixture conditions as compared to the rest of the fuels
- The flame speed of 50/50 blend was almost the same (1-3 cm/s higher) as that of conventional diesel at stoichiometric conditions

Another investigation done in this research was to see the effect of increasing the initial temperature of the mixture on flame speed, and the results are as follows.

- The flame speed of conventional diesel, GTL and 50/50 blend is increasing with the increase of initial temperature of the mixture
- The same has been reported in the literature for other alternative fuels, which established that GTL and the blended fuel is following regular trends

It was concluded that the trends obtained are reproducible but the quality of data can be further explored by chemical investigations. The GTL fuel can be a potential alternative fuel if the application requires higher flame speed near the stoichiometric conditions. Also, if the application required conserving conventional

diesel and using alternative fuel, 50/50 blend of conventional diesel and GTL shall give roughly the exact flame speeds.

## **6.2 Recommendations**

The following recommendations are suggested for future works on the developed test rig and future experimentations:

- It is recommended to insulate the steel outer surface of the test rig to ensure a steady temperature rise and drop inside the bomb.
- The fuel injection system of the test rig can be enhanced by using automotive fuel injectors. This will ensure proper spraying and atomization of fuel and accurate measure of fuel quantities being sprayed.
- It is recommended to investigate the fuels at different initial pressures and higher initial temperatures, but this should be done only after thoroughly accessing the test rig for safe operation.
- Different calculations models can be used to obtain the flame speeds and develop new correlations in the future
- Lastly, the test rig is capable of measuring flame speed by high speed imaging and for measuring turbulent flame speeds. This aspect of the test rig can be utilized in any future projects as Qatar University.



## REFERENCES

- [1] R. Costa and J. Sodre, "Compression ratio effects on an ethanol/gasoline fuelled engine performance," *Applied Thermal Engineering*, vol. 31, pp. 278-283, 2011.
- [2] H. Radhi, "Evaluating the potential impact of global warming on the UAE residential buildings - A contribution to reduce the CO2 emissions," *Building and environment*, vol. 44, no. 12, pp. 2451-2462, 2009.
- [3] Q. N. V. 2030, "Synthesis Report, General Secretariat of Development Planning," July 2008. [Online]. Available:  
[http://www2.gsdp.gov.qa/www1\\_docs/QNV2030\\_English\\_v2.pdf](http://www2.gsdp.gov.qa/www1_docs/QNV2030_English_v2.pdf). [Accessed 12 December 2014].
- [4] C. Whitson and A. Kuntadi, "Khuff Gas Condensate Development," in *International Petroleum Technology Conference*, Doha, 2005.
- [5] H. Sajjad, H. Masjuki, M. Varman, M. Kalam, M. Arbab, S. Imtenan and S. Ashrafur Rahman, "Engine combustion, performance and emission characteristics of gas to liquid (GTL) fuels and its blends with diesel and bio-

diesel," *Renewable and Sustainable Energy Reviews*, vol. 30, pp. 961-986, 2014.

- [6] IQ OG, "Gas to liquids-6 ground-breaking GTL," 2012.
- [7] A. S. Ibrahim and S. F. Ahmed, "Measurements of laminar flame speeds of alternative gaseous fuel mixtures," *ASME Journal of Energy Resources Technology*, vol. 137, no. 3, pp. 032209-1, 2015.
- [8] K. Agee, "Offshore advances. Fundamentals of gas to liquids," *London: Petroleum Economist*, pp. 30-31, 2005.
- [9] A. Mallik and V. Mantri, "Gas-to-liquids plants face challenges in the U.S. market," U.S. Energy Information Administration, 19 February 2014. [Online]. Available: <http://www.eia.gov/todayinenergy/detail.cfm?id=15071>. [Accessed 12 January 2015].
- [10] W. Al-Sachi, "Gas to liquids technology (GTL)," Scribd. N.p., 2006. [Online]. [Accessed March 2015].
- [11] P. Norton, K. Vertin, B. Bailey, N. Clark, D. Lyons and S. Goguen, "Emission from

- trucks using Fischer-Tropsch diesel fuel," *SAE paper*, vol. 982526, 1998.
- [12] T. Alleman and R. McCormick, "Fischer-Tropsch diesel fuels – properties and exhaust emissions: a literature review," *SAE paper*, vol. 763, 2003.
- [13] T. Alleman, L. Eudy and M. Miyasoto, "Fuel property, emission test, and operability results from a fleet of class 6 vehicles operating on gas-to-liquid fuel and catalyzed diesel particle filters," *SAE paper*, vol. 2959, 2004.
- [14] S. Turns, *An introduction to combustion*, Singapore: McGraw Hill, 2000.
- [15] J. Natarajan, T. Lieuwen and J. Seitzman, "Laminar flame speeds of  $H_2/CO$  mixtures: effect of  $CO_2$ , dilution, preheat temperature, and pressure," *Combustion and Flame*, vol. 1, p. 151, 2007.
- [16] J. Keck, "Turbulent Flame Structure and Speed," in *Nineteenth International Symposium on Combustion*, 1982.
- [17] A. Klimov, "Premixed turbulent flames interplay of hydrodynamic and chemical phenomena," *Dokl. Akad. Nauk*, vol. 20, pp. 56-59, 1975.

- [18] G. Andrews and D. Bradley, Determination of burning velocities: A critical review, American Elsevier Publishing Company, Inc., 1972.
- [19] F. Parsinejad, C. Arcari and H. Merghalchi, "Flame Structure and Burning Speed of JP-10 Air Mixtures," *Combustion Science and Technology*, vol. 178, pp. 975-1000, 2006.
- [20] F. Roper, "Laminar diffusion flame sizes for curved slot burners giving fan-shaped flames," *combustion and flame*, vol. 31, pp. 251-259, 1978.
- [21] R. Strehlow, Fundamentals of combustion, New York: McGraw-Hill, 1984.
- [22] R. Fristrom and A. Westenberg, Flame Structure, USA: McGraw-Hill, Inc., 1965.
- [23] C. Vagelopoulos and F. Egolfopoulos, "Direct experimental determination of laminar flame speeds," in *Twenty-seventh symposium (international) on combustion*, Los Angeles, 1998.
- [24] C. Almarcha, B. Denet and J. Quinard, "Premixed flames propagating freely in tubes," *Combustion and Flame*, vol. 162, no. 4, pp. 1225-1233, 2015.

- [25] J. Buffam and K. Cox, Measurement of Laminar Burning Velocity of Methane-Air Mixtures using a Slot and Bunsen Burner [Thesis], Worcester Polytechnic Institute, 2008.
- [26] A. Huzayyin, H. Moneib, M. Shehatta and A. Attia, "Laminar burning velocity and explosion index of LPG-air and propane-air mixtures," *Fuel*, vol. 87, no. 1, pp. 39-57, 2008.
- [27] D. Bradley and A. Mitcheson, "Mathematical solutions for explosions in spherical vessels," *Combustion and Flame*, vol. 26, pp. 201-217, 1976.
- [28] A. Dahoe, J. Zevenbergen, S. Lemkowitz and B. Scarlett, "Dust explosion in spherical vessels: the role of flame thickness in the validity of the cube-root law," *Journal of Loss Prevent Process Industries*, vol. 9, no. 1, pp. 33-44, 1996.
- [29] C. Rallis, A. Garforth and J. Steinz, "Laminar burning velocity of acetylene-air mixtures by the constant volume method: dependence on mixture composition, pressure and temperature," *Combustion and Flame*, vol. 9, pp. 354-356, 1965.
- [30] V. Babkin and Y. Kononenko, "Equations for determining normal flame velocity

in a constant-volume spherical bomb," *Combustion and Flame*, vol. 3, no. 2, pp. 268-275, 1967.

[31] M. Metghalchi and J. Keck, "Burning velocities of mixtures of air with methanol, isooctane, and indolene at high pressure and temperature," *Combustion and Flame*, vol. 48, pp. 191-210, 1982.

[32] D. Bradley, M. Lawes and M. Mansour, "Explosion bomb measurements of ethanol–air laminar gaseous flame characteristics at pressures up to 1.4MPa," *Combustion and Flame*, vol. 156, no. 7, pp. 1462-1470, 2009.

[33] D. Bradley, R. Hicks, M. Lawes, C. Sheppard and R. Woolley, "The Measurement of Laminar Burning Velocities and Markstein Numbers for Iso-octane–Air and Iso-octane–n-Heptane–Air Mixtures at Elevated Temperatures and Pressures in an Explosion Bomb," *Combustion and Flame*, vol. 115, no. 2, pp. 126-144, 1998.

[34] S. Ahmed, K. Kasti, B. Khalid and M. Olba, "Turbulent and Laminar Burning Velocity Measurements of New Alternative Fuels," QNRF-UREP 12-021-2-006, Doha, 2012.

- [35] M. Radwan, M. Ismail, S. Elfeky and O. Abu-Elyazeed, "Jojoba methyl ester as a diesel fuel substitute: Preparation and characterization," *Applied Thermal Engineering*, vol. 27, pp. 314-322, 2006.
- [36] B. Lewis and G. Von Elbe, *Combustion, Flames and Explosions of Gases*, 3rd ed., Academic Press, 1987.
- [37] C. Tung Chong and S. Hochgreb, "Measurements of laminar flame speeds of liquid fuels: Jet-A1, diesel, palm methyl esters and blends using particle imaging velocimetry (PIV)," *Proceedings of the Combustion Institute*, vol. 33, pp. 979-986, 2011.
- [38] N. Hashimoto, Y. Ozawa, N. Mori, I. Yuri and T. Hisamatsu, "Fundamental combustion characteristics of palm methyl ester (PME) as alternative fuel for gas turbines," *Fuel*, vol. 87, no. 15-16, pp. 3373-3378, 2009.
- [39] S. GTL, "Safety data sheet - shell GTL distillate," Shell Qatar, Doha, 2011.
- [40] Washington D.C.: The National Academies Press, 2011, p. 15.

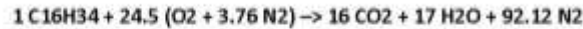
[41] J. Hansen, "Goddard Institute for Space Studies, GISS Surface Temperature Analysis," NASA Goddard Institute for Space Studies, 2006.



## APPENDIX A: MS EXCEL EQUIVALENCE RATIO CALCULATOR

### P1- Equivalence Ratio Calculations (Page 1/2)

The balanced chemical reaction for 1 mol of any Diesel is given by:



Mass of Fuel:	$m\text{-fuel} = n\text{-fuel} \times M.M\text{-fuel} = 1 \times M.M\text{-fuel}$ <b>m-fuel = 226 g</b>
Mass of Air:	$m\text{-air} = [n\text{-O}_2 \times M.M\text{-O}_2] + [n\text{-N}_2 \times M.M\text{-N}_2]$ $m\text{-air} = [n\text{-O}_2 \times M\text{-O}_2] + [n\text{-O}_2 \times (79/21) \times M\text{-N}_2]$ <b>m-air = 3364.67 g</b>
Air-Fuel Ratio (Stoic)	$(A/F)_{\text{stoic}} = m\text{-air}/m\text{-fuel} = 3364.67 / 226$ <b>(A/F)<sub>stoic</sub> = 14.89</b>
Equivalence Ratio	$\Phi = (A/F)_{\text{stoic}} / (A/F)_{\text{actual}}$ $\Phi = ???$

For  $(A/F)_{\text{actual}}$ , the actual amount of air in bomb and fuel injected will be considered.

Mass of Air in Bomb: (Method 1)	Bomb Vol = 0.1374 m <sup>3</sup>
	Density of air @ 180oC = 0.75 kg/m <sup>3</sup>
	Mass of air in bomb = m-air = <b>102.50 g</b>
	Molar Mass = M-air = 28.96 g/mol
	Moles = n-air = <b>3.54 mol</b>

Assuming Ideal Gas Case for Constant Volume of Air: (Method 2)

Temperature = T =	453.15 K
Ideal Gas Const. = R =	8.314 m <sup>3</sup> Pa/(mol K)
Bomb Volume = V =	0.1374 m <sup>3</sup>
Pressure = P =	101325 Pa
$n = (P V) / (R T)$	
Moles of Air = n-air =	<b>2.69 mol</b>
Mass of Air = m-air =	77.89 g

Mass of Fuel Injected in Bomb:	Vol-fuel = 6.5 mL
	Vol-fuel = 0.0000065 m <sup>3</sup>
	Density Fuel = 770000 g/m <sup>3</sup>
	<b>m-fuel = 5.005 g</b>

Since the O<sub>2</sub> sensor is reading a slightly lower %age of O<sub>2</sub> after injecting fuel, this means that total volume of bomb (air) is shared with some volume of fuel. Also, there is some air escaping the bomb through some leakage, reducing O<sub>2</sub>%. Therefore, the actual mass of air has to be calculated based on O<sub>2</sub> sensor reading now.

## P2- Equivalence Ratio Calculations (Page 2/2)

### O2 Sensor Readings and Actual Mass of Air

21% O2 means that 100 moles of Air has 21 moles of O2

Now, following table calculates the m-air for moles of air in bomb based on certain O2 % reading

O2 %	Total air in Bomb	Actual Mole of O2 (mol)	Actual Mass of Air (g)	V-Fuel Injected (mL)	m-fuel injected (g)	m-fuel evap (g)	(A/F) <sub>act</sub>	Φ =
20.4	3.54	0.72	99.18	5.0	3.85	3.43	28.91	0.5
20.3	3.54	0.72	98.69	5.3	4.08	3.93	25.10	0.6
20.2	3.54	0.72	98.20	6.0	4.62	4.43	22.15	0.7
20.1	3.54	0.71	97.72	6.5	5.01	4.94	19.80	0.8
19.9	3.54	0.70	96.75	8.0	6.16	5.94	16.29	0.9
19.8	3.54	0.70	96.26	9.0	6.93	6.44	14.94	1.0
19.7	3.54	0.70	95.77	9.3	7.16	6.94	13.79	1.1
19.6	3.54	0.69	95.29	10.0	7.70	7.45	12.80	1.2

### Sample Calculation from above table, at O2% = 19.8%

O2 Sensor Reading = 19.8%  
 moles of air in bomb = n-air = 3.54 mol  
 moles of O2 actual = n-O2 = 0.701 mol  
 mass of Air actual = m-air = 96.25968 g

Vol of fuel injected v-fuel = 6.5 mL  
 v-fuel = 6.5E-06 m3  
 Mass of fuel injected m-fuel = 5.005 g

### Actual Vol of Fuel shared with Air

density of air = 0.75 kg/m3  
 Vol-Air left in bomb after fuel injection = m-air actual x density of air  
 V-Air Actual = 0.129 m3  
 Vol fuel shared with Air = (Bomb Volume) - (V-Air actual)  
 V-fuel actual = 0.008 m3  
 m-fuel actual = 6.44 g

Air-Fuel Ratio Actual (A/F)<sub>act</sub> = 14.94 g

Equivalence Ratio  $\Phi = (A/F)_{\text{stoic}} / (A/F)_{\text{actual}}$

$$\Phi = 1.00$$

## APPENDIX B: MS EXCEL FLAME CALCULATOR

### P2- Laminar Burning Velocity Calculations

Equation to use:  $S_{li} = (dr/dt) (ri/rb)^2 (pi/p)^{1/\gamma_u}$   
 Lewis and Von [23]

- Eq (i)  $dr/dt = (R/3(P_e - P_i)) \{ [(P_e - P_i)/(P_e - P_i)]^{2/3} (dp/dt) \}$   
 Eq (ii)  $r_i = R \{ [P_e - P_i / (P_e - P_i)]^{1/3} \}$   
 Eq (iii)  $n_i = R \{ [1 - (P_e/P_i)] (T_u/T_i) \} (P_e - P_i) / (P_e - P_i) \}$   
 Eq (iv)  $(T_u/T_i) = (P_e/P_i)^{1/\gamma_u}$

Test Fuel: Diesel at 190 oC								
Parameter	Symbol (Units)	$\Phi = 0.7$	$\Phi = 0.8$	$\Phi = 0.9$	$\Phi = 1.0$	$\Phi = 1.1$	$\Phi = 1.2$	$\Phi = 1.3$
Radius of Bomb	R (m)	0.4	0.4	0.4	0.4	0.4	0.4	0.4
Pressure - Initial before combustion	Pi (Bar)	1.1	1.1	1.1	1.1	1.1	1.1	1.1
Pressure - Initial before combustion	Pi (Pa)	110000	110000	110000	110000	110000	110000	110000
Pressure - Equilibrium Burned Gases	Pe (Bar)	1.13	1.13	1.13	1.13	1.13	1.13	1.13
Pressure - Equilibrium Burned Gases	Pe (Pa)	113000	113000	113000	113000	113000	113000	113000
Pressure - Peak during combustion	P (Bar)	2.29	2.9	3.27	3.58	4.02	3.95	3.9
Pressure - Peak during combustion	P (Pa)	229000	290000	327000	358000	402000	395000	390000
Temperature - Burned Gas	Tu (oC)	210	210	210	210	210	210	210
Temperature - Burned Gas	Tu (K)	484.15	484.15	484.15	484.15	484.15	484.15	484.15
Temperature - Initial Mixture	Ti (oC)	180	180	180	180	180	180	180
Temperature - Initial Mixture	Ti (K)	454.15	454.14	454.14	454.14	454.14	454.14	454.14
Slope - Pressure vs. Time Curve	(dp/dt)	36.90	36.9	36.9	36.9	36.9	36.9	36.9
1st Equation	dr/dt	0.47	0.61	0.69	0.76	0.85	0.83	0.82
2nd Equation	ri	1.36	1.57	1.67	1.74	1.84	1.83	1.81
3rd Equation	rb	8.32	9.94	10.63	11.10	11.64	11.56	11.51
4th Equation	(p/pi) <sup>1/γu</sup>	1.07	1.07	1.07	1.07	1.07	1.07	1.07
Laminar Flame Speed	S <sub>li</sub> (m/s)	0.49	0.60	0.67	0.74	0.83	0.82	0.81
Laminar Flame Speed	S <sub>li</sub> (cm/s)	49.20	59.81	67.12	73.58	83.19	81.63	80.52

## APPENDIX C: CALIBRATION CERTIFICATES



**Environmental Equipment, Inc.**

3634 Central Ave. St. Petersburg, Florida 33711 · Phone 727-328-2818 · FAX 727-328-2826 · E-mail: sales@imrusa.com

### Certificate of Calibration

<b>Customer:</b> Qatar University <b>Address:</b> Samahat Samim P.O. Box 2713, Doha Ad Dawha, Qatar <b>Model #</b> IMR1000-1 <b>Serial #</b> A4905A67	<b>Calibration Date:</b> August 13, 2014 <b>Expiration Date:</b> August 13, 2015 <b>Temperature:</b> 20 C <b>Atmospheric Pressure:</b> 1013 hPA <b>Relative Humidity:</b> 55%
--	---

Calibration Gas	Bottle Serial Number	Preparation Date	Stability
O2	X02N190C2003081	7/23/2013	24 months

*Air Gas is the manufacturer of all calibration gases that are traceable to NIST.*

### Calibration Data

Gas	Unit	Range	Standard	Measured	Tolerance	Accepted Tolerance
O2	%	20.9	9.97	10.1	0.13	± 0.21

**Calibrated By:** Branden Baker

**Signature:**

**Inspected By:** Gustavo Maturana

**Signature:**

**Date:** August 13, 2014





~ Calibration Certificate ~

Model Number: 422E35 Customer: \_\_\_\_\_  
Serial Number: 43787 \_\_\_\_\_  
Description: Charge Converter P.O.: \_\_\_\_\_  
Manufacturer: PCB Method: Comparison Method (AT-119-2)

**Calibration Data**

Temperature: 72 °F ( 22 °C) Humidity: 57%

**Input Parameters :**

Frequency 100 Hz Source Capacitance 993.79 pF

**Test Results:**


Gain: 0.990 mV/pC Bias Voltage: 13.99 VDC

**Condition of Unit**

As Found: n/a  
As Left: New unit, in tolerance

**Notes**

1. This inverting charge amplifier has a fixed gain, range and feedback resistance.
2. Calibration is N.I.S.T. traceable through PCB control number QC-214.
3. This certificate shall not be reproduced, except in full, without written approval from PCB Piezotronics, Inc.
4. Calibration is performed in compliance with ISO 9001, ISO 10012-1, ANSE/NCCL Z540.3 and ISO 17025.
5. Measurement uncertainty (95% confidence level with a coverage factor of 2) for the sensitivity reading is +/- 0.2 %
6. See Manufacturer's Specification Sheet for a detailed listing of performance specifications.

Technician: Mark Moorhouse 

Date: 6/9/2015

Due Date: \_\_\_\_\_



CALIBRATION CERT #1862.01

 **PCB PIEZOTRONICS™**

3425 Walden Avenue  
Depew, New York 14043

TEL: 888-684-0013

FAX: 716-685-3886

www.pcb.com

ILE22-3516720911

# APPENDIX D: GTL MSDS

Shell GTL Distillate  
Version 1.5  
Effective Date 03.11.2011

## Safety Data Sheet

heated above the flash point. Do not puncture, cut or weld uncleaned drums. Do not pollute the soil, water or environment with the waste container. Comply with any local recovery or waste disposal regulations.

**Local Legislation** : Disposal should be in accordance with applicable regional, national, and local laws and regulations. Local regulations may be more stringent than regional or national requirements and must be complied with.

---

## 14. TRANSPORT INFORMATION

### Land (as per ADR classification): Regulated

Class : 3  
Packing group : III  
Hazard identification no. : 30  
UN No. : 1202  
Danger label (primary risk) : 3  
Proper shipping name : GAS OIL

### IMDG

This material is not classified as dangerous under IMDG regulations.

### IATA (Country variations may apply)

This material is either not classified as dangerous under IATA regulations or needs to follow country specific requirements.

**Additional Information** : MARPOL Annex 1 rules apply for bulk shipments by sea. This product is being carried under the scope of MARPOL Annex I.

Special Precautions: Refer to Chapter 7, Handling & Storage, for special precautions which a user needs to be aware of or needs to comply with in connection with transport.

---

## 15. REGULATORY INFORMATION

The regulatory information is not intended to be comprehensive. Other regulations may apply to this material.

**Classification triggering components** : Contains distillates (Fischer Tropsch), C8 - C26 branched and linear alkanes.

---

## 16. OTHER INFORMATION

**Additional Information** : This document contains important information to ensure the safe storage, handling and use of this product. The information in this document should be brought to the attention of the

---

Print Date 03.11.2011 10/11 00000021991  
MSDS\_IMO



## Safety Data Sheet

<b>Developmental Toxicity</b>	
<b>Specific target organ toxicity - single exposure</b>	: High concentrations may cause central nervous system depression resulting in headaches, dizziness and nausea; continued inhalation may result in unconsciousness and/or death.
<b>Specific target organ toxicity - repeated exposure</b>	: Not expected to be a hazard.

---

### 12. ECOLOGICAL INFORMATION

<b>Basis for Assessment</b>	: Information given is based on product data, a knowledge of the components and the ecotoxicology of similar products.
<b>Acute Toxicity</b>	: Expected to be practically non toxic; LL/EL/IL50 > 100 mg/l (to aquatic organisms) (LL/EL50 expressed as the nominal amount of product required to prepare aqueous test extract).
<b>Mobility</b>	: Floats on water. Partly evaporates from water or soil surfaces, but a significant proportion will remain after one day. Large volumes may penetrate soil and could contaminate groundwater.
<b>Persistence/degradability</b>	: Not Persistent per IMO criteria. International Oil Pollution Compensation (IOPC) Fund definition: "A non-persistent oil is oil, which, at the time of shipment, consists of hydrocarbon fractions, (a) at least 50% of which, by volume, distills at a temperature of 340°C (645°F) and (b) at least 95% of which, by volume, distills at a temperature of 370°C (700°F) when tested by the ASTM Method D-86/78 or any subsequent revision thereof." Readily biodegradable.
<b>Bioaccumulative Potential</b>	: Contains constituents with the potential to bioaccumulate.
<b>Other Adverse Effects</b>	: Films formed on water may affect oxygen transfer and damage organisms.

---

### 13. DISPOSAL CONSIDERATIONS

<b>Material Disposal</b>	: Recover or recycle if possible. It is the responsibility of the waste generator to determine the toxicity and physical properties of the material generated to determine the proper waste classification and disposal methods in compliance with applicable regulations. Do not dispose into the environment, in drains or in water courses. Do not dispose of tank water bottoms by allowing them to drain into the ground. This will result in soil and groundwater contamination. Waste arising from a spillage or tank cleaning should be disposed of in accordance with prevailing regulations, preferably to a recognised collector or contractor. The competence of the collector or contractor should be established beforehand.
<b>Container Disposal</b>	: Send to drum recoverer or metal reclaimer. Drain container thoroughly. After draining, vent in a safe place away from sparks and fire. Residues may cause an explosion hazard if

## Safety Data Sheet

<b>Kinematic viscosity</b>	: 1.8 - 4.5 mm <sup>2</sup> /s at 40 °C / 104 °F
<b>Vapour density (air=1)</b>	: > 5
<b>Evaporation rate (nBuAc=1)</b>	: Data not available
<b>Flammability</b>	: Combustible liquid.

---

### 10. STABILITY AND REACTIVITY

<b>Chemical Stability</b>	: Stable under normal conditions of use.
<b>Possibility of Hazardous Reactions</b>	: Data not available
<b>Conditions to Avoid</b>	: Avoid heat, sparks, open flames and other ignition sources.
<b>Incompatible Materials</b>	: Strong oxidising agents.
<b>Hazardous Decomposition Products</b>	: Hazardous decomposition products are not expected to form during normal storage. Thermal decomposition is highly dependent on conditions. A complex mixture of airborne solids, liquids and gases, including carbon monoxide, carbon dioxide and other organic compounds will be evolved when this material undergoes combustion or thermal or oxidative degradation.

---

### 11. TOXICOLOGICAL INFORMATION

<b>Basis for Assessment</b>	: Information given is based on product data, a knowledge of the components and the toxicology of similar products.
<b>Likely Routes of Exposure</b>	: Inhalation is the primary route of exposure although absorption may occur through skin contact or following accidental ingestion.
<b>Acute Oral Toxicity</b>	: Low toxicity: LD50 > 5000 mg/kg , Rat
<b>Acute Dermal Toxicity</b>	: Expected to be of low toxicity: LD50 >2000 mg/kg , Rabbit
<b>Acute Inhalation Toxicity</b>	: Expected to be of low toxicity: LC50 >5 mg/l , 4 h, Rat
<b>Skin Corrosion/Irritation</b>	: Expected to be slightly irritating. Prolonged/repeated contact may cause defatting of the skin which can lead to dermatitis.
<b>Serious Eye Damage/Irritation</b>	: Expected to be slightly irritating.
<b>Respiratory Irritation</b>	: Expected to be slightly irritating.
<b>Respiratory or Skin Sensitisation</b>	: Not expected to be a sensitiser.
<b>Aspiration Hazard</b>	: Aspiration into the lungs when swallowed or vomited may cause chemical pneumonitis which can be fatal.
<b>Germ Cell Mutagenicity</b>	: Not mutagenic.
<b>Carcinogenicity</b>	: Not a carcinogen.
<b>Reproductive and</b>	: Not a developmental toxicant. Does not impair fertility.

## Safety Data Sheet

	appropriate positive pressure breathing apparatus. Where air-filtering respirators are suitable, select an appropriate combination of mask and filter. All respiratory protection equipment and use must be in accordance with local regulations.
<b>Hand Protection</b>	: Personal hygiene is a key element of effective hand care. Gloves must only be worn on clean hands. After using gloves, hands should be washed and dried thoroughly. Application of a non-perfumed moisturizer is recommended. Suitability and durability of a glove is dependent on usage, e.g. frequency and duration of contact, chemical resistance of glove material, glove thickness, dexterity. Always seek advice from glove suppliers. Contaminated gloves should be replaced. Select gloves tested to a relevant standard (e.g. Europe EN374, US F739). When prolonged or frequent repeated contact occurs, Nitrile gloves may be suitable. (Breakthrough time of > 240 minutes.) For incidental contact/splash protection Neoprene, PVC gloves may be suitable.
<b>Eye Protection</b>	: Chemical splash goggles (chemical monogoggles).
<b>Protective Clothing</b>	: Chemical resistant gloves/gauntlets, boots, and apron (where risk of splashing).
<b>Thermal Hazards</b>	: Not applicable.
<b>Monitoring Methods</b>	: Monitoring of the concentration of substances in the breathing zone of workers or in the general workplace may be required to confirm compliance with an OEL and adequacy of exposure controls. For some substances biological monitoring may also be appropriate.
<b>Environmental Exposure Controls</b>	: Local guidelines on emission limits for volatile substances must be observed for the discharge of exhaust air containing vapour.

## 9. PHYSICAL AND CHEMICAL PROPERTIES

<b>Appearance</b>	: Colourless. Liquid.
<b>Odour</b>	: Data not available
<b>Odour threshold</b>	: Data not available
<b>pH</b>	: Data not available
<b>Initial Boiling Point and Boiling Range</b>	: 160 - 360 °C / 320 - 680 °F
	:
<b>Flash point</b>	: > 75 °C / 167 °F
<b>Upper / lower Flammability or Explosion limits</b>	: 0.5 - 5.0 %(V)
<b>Auto-ignition temperature</b>	: > 215 °C / 419 °F
<b>Vapour pressure</b>	: < 0.1 kPa at 25 °C / 77 °F
<b>Relative Density</b>	: 0.77
<b>Density</b>	: Typical 0.77 g/cm <sup>3</sup> at 15 °C / 59 °F
<b>Water solubility</b>	: Negligible.
<b>Solubility in other solvents</b>	: Data not available
<b>n-octanol/water partition coefficient (log Pow)</b>	: > 6.5
<b>Dynamic viscosity</b>	: Data not available

## Safety Data Sheet

<b>Unsuitable Materials</b>	: amine-adduct cured epoxy paint. For seals and gaskets use: graphite, PTFE, Viton A, Viton B. : Some synthetic materials may be unsuitable for containers or container linings depending on the material specification and intended use. Examples of materials to avoid are: natural rubber (NR), nitrile rubber (NBR), ethylene propylene rubber (EPDM), polymethyl methacrylate (PMMA), polystyrene, polyvinyl chloride (PVC), polyisobutylene. However, some may be suitable for glove materials.
<b>Container Advice</b>	: Containers, even those that have been emptied, can contain explosive vapours. Do not cut, drill, grind, weld or perform similar operations on or near containers.
<b>Other Advice</b>	: Ensure that all local regulations regarding handling and storage facilities are followed.

---

## 8. EXPOSURE CONTROLS/PERSONAL PROTECTION

If the American Conference of Governmental Industrial Hygienists (ACGIH) value is provided on this document, it is provided for information only.

None established.

### Occupational Exposure Limits

**Additional Information** : In the absence of a national exposure limit, the American Conference of Governmental Industrial Hygienists (ACGIH) recommends the following values for Diesel Fuel: TWA - 100 mg/m<sup>3</sup> Critical effects based on Skin and Irritation.

**Biological Exposure Index (BEI) - See reference for full details**  
No biological limit allocated.

**Appropriate Engineering Controls** : The level of protection and types of controls necessary will vary depending upon potential exposure conditions. Select controls based on a risk assessment of local circumstances.  
Appropriate measures include: Use sealed systems as far as possible. Adequate ventilation to control airborne concentrations below the exposure guidelines/limits. Local exhaust ventilation is recommended. Eye washes and showers for emergency use.

**Individual Protection Measures** : Personal protective equipment (PPE) should meet recommended national standards. Check with PPE suppliers.

**Respiratory Protection** : If engineering controls do not maintain airborne concentrations to a level which is adequate to protect worker health, select respiratory protection equipment suitable for the specific conditions of use and meeting relevant legislation. Check with respiratory protective equipment suppliers. Where air-filtering respirators are unsuitable (e.g. airborne concentrations are high, risk of oxygen deficiency, confined space) use

## Safety Data Sheet

Chapter 8 of this Material Safety Data Sheet. Use the information in this data sheet as input to a risk assessment of local circumstances to help determine appropriate controls for safe handling, storage and disposal of this material. Air-dry contaminated clothing in a well-ventilated area before laundering. Properly dispose of any contaminated rags or cleaning materials in order to prevent fires. Prevent spillages. Use local exhaust ventilation if there is risk of inhalation of vapours, mists or aerosols. Never siphon by mouth. Contaminated leather articles including shoes cannot be decontaminated and should be destroyed to prevent reuse. For comprehensive advice on handling, product transfer, storage and tank cleaning refer to the product supplier. Maintenance and Fuelling Activities - Avoid inhalation of vapours and contact with skin.

**Precautions for Safe Handling**

: Avoid inhaling vapour and/or mists. Avoid prolonged or repeated contact with skin. When using do not eat or drink. Extinguish any naked flames. Do not smoke. Remove ignition sources. Avoid sparks. Earth all equipment. Electrostatic charges may be generated during pumping. Electrostatic discharge may cause fire. Not expected to be a health hazard when used under normal conditions. The vapour is heavier than air, spreads along the ground and distant ignition is possible.

**Conditions for Safe Storage**

: Drum and small container storage: Drums should be stacked to a maximum of 3 high. Use properly labelled and closeable containers. Tank storage: Tanks must be specifically designed for use with this product. Bulk storage tanks should be diked (bunded). Locate tanks away from heat and other sources of ignition. Must be stored in a diked (bunded) well-ventilated area, away from sunlight, ignition sources and other sources of heat. The vapour is heavier than air. Beware of accumulation in pits and confined spaces. Keep in a bunded area with a sealed (low permeability) floor, to provide containment against spillage. Prevent ingress of water.

**Product Transfer**

: Avoid splash filling. Wait 2 minutes after tank filling (for tanks such as those on road tanker vehicles) before opening hatches or manholes. Wait 30 minutes after tank filling (for large storage tanks) before opening hatches or manholes. Keep containers closed when not in use. Do not use compressed air for filling, discharging or handling. Contamination resulting from product transfer may give rise to light hydrocarbon vapour in the headspace of tanks that have previously contained gasoline. This vapour may explode if there is a source of ignition. Partly filled containers present a greater hazard than those that are full, therefore handling, transfer and sampling activities need special care.

**Recommended Materials**

: For containers, or container linings use mild steel, stainless steel. Aluminium may also be used for applications where it does not present an unnecessary fire hazard. Examples of suitable materials are: high density polyethylene (HDPE) and Viton (FKM), which have been specifically tested for compatibility with this product. For container linings, use

## Safety Data Sheet

- Protective Equipment & Precautions for Fire Fighters** : Wear full protective clothing and self-contained breathing apparatus.
- Additional Advice** : Keep adjacent containers cool by spraying with water.

---

### 6. ACCIDENTAL RELEASE MEASURES

Avoid contact with spilled or released material. For guidance on selection of personal protective equipment see Chapter 8 of this Material Safety Data Sheet. See Chapter 13 for information on disposal. Observe the relevant local and international regulations. Evacuate the area of all non-essential personnel. Ventilate contaminated area thoroughly.

- Personal Precautions, Protective Equipment and Emergency Procedures** : Do not breathe fumes, vapour. Do not operate electrical equipment.
- Environmental Precautions** : Shut off leaks, if possible without personal risks. Remove all possible sources of ignition in the surrounding area. Use appropriate containment (of product and fire fighting water) to avoid environmental contamination. Prevent from spreading or entering drains, ditches or rivers by using sand, earth, or other appropriate barriers. Attempt to disperse the vapour or to direct its flow to a safe location for example by using fog sprays. Take precautionary measures against static discharge. Ensure electrical continuity by bonding and grounding (earthing) all equipment.
- Methods and Material for Containment and Clean Up** : For small liquid spills (< 1 drum), transfer by mechanical means to a labelled, sealable container for product recovery or safe disposal. Allow residues to evaporate or soak up with an appropriate absorbent material and dispose of safely. Remove contaminated soil and dispose of safely.  
For large liquid spills (> 1 drum), transfer by mechanical means such as vacuum truck to a salvage tank for recovery or safe disposal. Do not flush away residues with water. Retain as contaminated waste. Allow residues to evaporate or soak up with an appropriate absorbent material and dispose of safely. Remove contaminated soil and dispose of safely. Shovel into a suitable clearly marked container for disposal or reclamation in accordance with local regulations.
- Additional Advice** : Notify authorities if any exposure to the general public or the environment occurs or is likely to occur. Local authorities should be advised if significant spillages cannot be contained. Maritime spillages should be dealt with using a Shipboard Oil Pollution Emergency Plan (SOPEP), as required by MARPOL Annex 1 Regulation 26.

---

### 7. HANDLING AND STORAGE

- General Precautions** : Avoid breathing vapours or contact with material. Only use in well ventilated areas. Wash thoroughly after handling. For guidance on selection of personal protective equipment see

## Safety Data Sheet

Chemical Identity	CAS	Conc.
Distillates (Fischer-Tropsch) C8-26 - Branched and Linear	848301-67-7	100.00 %

### 4. FIRST AID MEASURES

<b>Inhalation</b>	: Remove to fresh air. If rapid recovery does not occur, transport to nearest medical facility for additional treatment.
<b>Skin Contact</b>	: Remove contaminated clothing. Immediately flush skin with large amounts of water for at least 15 minutes, and follow by washing with soap and water if available. If redness, swelling, pain and/or blisters occur, transport to the nearest medical facility for additional treatment.
<b>Eye Contact</b>	: Flush eye with copious quantities of water. If persistent irritation occurs, obtain medical attention.
<b>Ingestion</b>	: If swallowed, do not induce vomiting; transport to nearest medical facility for additional treatment. If vomiting occurs spontaneously, keep head below hips to prevent aspiration. If vomiting occurs spontaneously, keep head below hips to prevent aspiration. If any of the following delayed signs and symptoms appear within the next 6 hours, transport to the nearest medical facility: fever greater than 101°F (38.3°C), shortness of breath, chest congestion or continued coughing or wheezing.
<b>Most Important Symptoms/Effects, Acute &amp; Delayed</b>	: If material enters lungs, signs and symptoms may include coughing, choking, wheezing, difficulty in breathing, chest congestion, shortness of breath, and/or fever. The onset of respiratory symptoms may be delayed for several hours after exposure. Defatting dermatitis signs and symptoms may include a burning sensation and/or a dried/cracked appearance.
<b>Immediate medical attention, special treatment</b>	: Treat symptomatically.

### 5. FIRE FIGHTING MEASURES

Clear fire area of all non-emergency personnel.

<b>Specific hazards arising from Chemicals</b>	: Hazardous combustion products may include: A complex mixture of airborne solid and liquid particulates and gases (smoke). Carbon monoxide. Unidentified organic and inorganic compounds. Carbon monoxide may be evolved if incomplete combustion occurs. Will float and can be reignited on surface water. Flammable vapours may be present even at temperatures below the flash point.
<b>Suitable Extinguishing Media</b>	: Foam, water spray or fog. Dry chemical powder, carbon dioxide, sand or earth may be used for small fires only.
<b>Unsuitable Extinguishing Media</b>	: Do not use water in a jet.

## Safety Data Sheet

<b>Storage</b>	: P403+P235: Store in a well-ventilated place. Keep cool. P405: Store locked up.
<b>Disposal</b>	: P501: Dispose of contents and container to appropriate waste site or reclaimer in accordance with local and national regulations.
<b>Other Hazards which do not result in classification</b>	: Slightly irritating to respiratory system. Breathing of high vapour concentrations may cause central nervous system (CNS) depression resulting in dizziness, light-headedness, headache and nausea. May cause slight irritation to skin. Repeated exposure may cause skin dryness or cracking. May ignite on surfaces at temperatures above auto-ignition temperature. Vapour in the headspace of tanks and containers may ignite and explode at temperatures exceeding auto-ignition temperature, where vapour concentrations are within the flammability range. Electrostatic charges may be generated during pumping. Electrostatic discharge may cause fire.
<b>Additional Information</b>	: This product is intended for use in closed systems only.

---

### 3. COMPOSITION/INFORMATION ON INGREDIENTS

<b>Preparation Description</b>	: A complex combination of hydrocarbons obtained from a feedstock derived from the catalytic hydrogenation of carbon monoxide (the Fischer - Tropsch Process), optionally followed by one or more of the following processes: hydrotreatment, hydroisomerisation, hydrocracking. It consists predominantly of branched and linear aliphatic hydrocarbons having carbon numbers in the range of C8 to C26 and boiling in the range of approximately 120C to 380C (248F to 716F).
<b>Synonyms</b>	: Shell GTL Fuel Shell GTL Gasoil Heavy Normal Paraffin Shell GTL Sarasol 100 Hydrocarbon Solvent 108 Liquid Paraffin 100 Mixed Paraffin 360 Paraffin Oil Paraffin Oil W Paraffin Oil (Liquid Paraffin) C12 - C22 Shell GTL Saraline 200 Shell GTL Saraline 98V Shell GTL Saraline 185V Liquid Paraffin 85 Shell GTL Sarasol 85 ISO N-Paraffins Shell GTL Light Fuel Liquid Paraffins - H Paraffin Oil - H
<b>Hazardous Components</b>	



## Safety Data Sheet

### 1. IDENTIFICATION OF THE SUBSTANCE/PREPARATION AND COMPANY/UNDERTAKING

<b>Material Name</b>	: Shell GTL Distillate
<b>Other Names / Synonyms</b>	: Shell GTL Fuel
<b>Recommended Use / Restrictions of Use</b>	: Alkanes, middle distillate-range, hydrotreated. / Automotive gasoil blending component.
<b>Supplier</b>	: Shell Trading Rotterdam B.V. Weena 70 3012 CM Rotterdam Netherlands
<b>Contact Telephone</b>	: +31 10 441 5000
<b>Emergency Telephone Number</b>	: +1 703-527-3887
<b>MARPOL Annex I Category</b>	: Gas Oils (including ship's bunkers)
<b>Description on Bill of Lading (B/L)/Bunker delivery note/Shipping document</b>	: Distillates (Annex 1, Appendix 1 Name)
<b>Other Information</b>	: See Section 14 for transportation information related to the Bill of Lading, other shipping documents.

### 2. HAZARDS IDENTIFICATION

<b>GHS Classification</b>	: FLAMMABLE LIQUIDS, Category 4 ASPIRATION HAZARD, Category 1
<b>GHS Label Elements Symbol(s)</b>	: 
<b>Hazard Statement</b>	: PHYSICAL HAZARDS: H227: Combustible liquid.
<b>Signal Words</b>	: Danger HEALTH HAZARDS: H304: May be fatal if swallowed and enters airways.
<b>GHS Precautionary Statements</b>	
<b>Prevention</b>	: P210: Keep away from heat/sparks/open flames/hot surfaces. - No smoking. P280: Wear protective gloves/protective clothing/eye protection/face protection.
<b>Response</b>	: P301+P310: IF SWALLOWED: Immediately call a POISON CENTER or doctor/physician. P331: Do NOT induce vomiting.

## Safety Data Sheet

	person in your organisation responsible for advising on safety matters.
<b>MSDS Version Number</b>	: 1.5
<b>MSDS Effective Date</b>	: 03.11.2011
<b>MSDS Revisions</b>	: A vertical bar ( ) in the left margin indicates an amendment from the previous version.
<b>Uses and Restrictions</b>	: This product must not be used in applications other than those recommended in Section 1, without first seeking the advice of the supplier.
<b>MSDS Distribution</b>	: The information in this document should be made available to all who may handle the product.
<b>Disclaimer</b>	: This information is based on our current knowledge and is intended to describe the product for the purposes of health, safety and environmental requirements only. It should not therefore be construed as guaranteeing any specific property of the product.